The transcriptomic signature of age and sex is not conserved in human primary myocytes

Running title: Age and sex traits are not conserved in myocytes

Séverine Lamon[1], Megan Soria[2], Ross Williams[1], Annabel Critchlow[1], Andrew Garnham[1], Akriti Varshney[3], Traude Beillharz[3], Danielle Hiam[1] and Mark Ziemann[4]

[1]Institute for Physical Activity and Nutrition, School of Exercise and Nutrition Sciences, Deakin University, Geelong, Australia

[2]School of Life and Environmental Sciences, Deakin University, Geelong, Australia

[3]Development and Stem Cells Program, Monash Biomedicine Discovery Institute and Department of Biochemistry and Molecular Biology, Monash University, Melbourne, Australia

[4]Bioinformatics Working Group, Burnet Institute, Melbourne, Australia

severine.lamon@deakin.edu.au

msoria@deakin.edu.au

s222563742@deakin.edu.au

s222618693@deakin.edu.au

andrew.garnham@deakin.edu.au

akriti.varshney@monash.edu

traude.beilharz@monash.edu

danielle.hiam@deakin.edu.au

mark.ziemann@burnet.edu.au

Character count (including blanks, excluding references): 46,251

Ethics statement: This research study was granted ethical approval by the Deakin University Human Research Ethics Committee (DUHREC 2021-307).

Abstract

Human primary muscle cell (HPMC) lines derived from skeletal muscle biopsies are potentially powerful tools to interrogate the molecular pathways underlying fundamental muscle mechanisms. HPMCs retain their genome in culture, but many endogenous circulating factors are not present in the *in vitro* environment or at concentrations that do not mirror physiological levels. To address the assumption that HPMCs are valid models of age and sex-specificity in human muscle research, we examined to what extent HPMC lines maintain their source phenotypes in culture. A comparison of the transcriptomic signature of 30 human muscle biopsies (N = 10 young males, N = 10 young females, N = 10 old males) and their corresponding HPMCs indicated a near-complete lack of retention of the genes and pathways that were differentially regulated *in vivo* when compared to their *in vitro* equivalent, except for some genes encoded on the Y-chromosome. The diversity of the muscle cell population and the lack of sex- and age-dependent factors in the cellular milieu likely contribute to these observations, which call for caution when using HPMCs as an experimental model of human muscle sex or age. Nuclear single cell sequencing or HMPCs grown in 3D culture as organoids under strain might therefore provide a closer alternative to human muscle tissue.

Keywords: Aging; Sex; Transcriptome; Muscle Cells; Primary Cell Culture

Introduction

Skeletal muscle is essential to human posture, movement and metabolism and is a critical component of healthy ageing (Tieland et al., 2018). Primary muscle cell lines (Blau & Webster, 1981) established from human or rodent muscle tissue are potentially powerful tools to interrogate the molecular pathways underlying fundamental muscle mechanisms. The phenotype of a cell line can be modified using molecular tools that may or may not alter its genotype, which reduces the number of animals used in research and is cheaper and faster than animal experiments. Primary muscle cell lines provide an alternative to the traditional C_2C_{12} line, an immortalized murine myoblast derived cell line (Burattini et al., 2004) with cycles of 'active' to 'resting' that closely resembles those of satellite cells that cycle between an activated and a quiescent state (Yoshida et al., 1998). While complex to establish (Blau & Webster, 1981), more expensive to maintain and limited in the number of times they can be passaged, human primary muscle cell (HPMC) lines may be molecularly and metabolically closer to human physiology (Abdelmoez et al., 2020) despite their intrinsic genetic heterogeneity.

Skeletal muscle is one of the most sex-biased tissues of the body (Oliva et al., 2020). At baseline, it has up to 3000 genes that are differentially expressed in males and females (Oliva et al., 2020), contributing to numerous sex-specific phenotypic traits, for example in muscle growth (Deasy et al., 2007), regenerative capacity (Deasy et al., 2007) and fibre type distribution (Haizlip et al., 2015) (see (Landen et al., 2021) for a full review). It follows that many fundamental mechanisms underlying skeletal muscle biology are sex-specific and cannot be inferred from single- or combined-sex study designs. Skeletal muscle is also profoundly affected by ageing, which facilitates an irregular yet progressive series of molecular and cellular dysfunctions that inevitably impact muscle structure, function and metabolism (Arentson-Lantz et al., 2020; Arentson-Lantz et al., 2021; Lamon et al., 2016; Lee et al., 2024; Seale et al., 2022; Zacharewicz et al., 2014). A common, directly observable consequence is age-related muscle loss; an insidious, progressive process characterized by 3–8% reduction in muscle mass and function per decade from the fifth decade ~~of age~~ (English & Paddon-Jones, 2010). At the transcriptome level, recent studies highlight the pathways deregulated during ageing (Schaiter et al., 2024; Tumasian et al., 2021), which were largely similar in males and

females despite sex differences in individual gene expression (Gharpure et al., 2023) and magnitude of the changes (de Jong et al., 2023).

HPMC lines retain the genome of their donor in culture, including some of the differences due to the sex chromosome complement (Wijchers et al., 2010; Zore et al., 2018), with primary differences in gene expression and DNA methylation (Davegårdh et al., 2019). Primary cultures allow tight control of the micro-environment of cells. Many endogenous circulating factors, including sex- and age-dependent factors such as steroid hormones and growth factors, are however either not present in the *in vitro* environment or at concentrations that do not mirror physiological levels. Whether and to what extent HPMC lines maintain their source phenotypes in culture is therefore in need of full examination. For example, we and others showed that some of the 'ageing' phenotypes of the myocytes derived from old subjects are lost in cell culture models (Alsharidah et al., 2013; Conboy et al., 2005; Zacharewicz et al., 2020), while other age- and metabolism-related traits that are partially conserved may include lipolysis, insulin sensitivity (Kase et al., 2015) and DNA methylation (Turner et al., 2020). The same applies to male and female derived cell lines (Davegårdh et al., 2019). While some sex differences may be conserved in HPMCs, the extent of the sex differences mediated by gonadal sex hormones that is retained in culture is unknown.

Regardless of these limitations, HPMCs are commonly used to probe age and sex-specific muscle molecular pathways in the muscle literature. To address the assumption that HPMCs are valid models of age and sex-specificity, we conducted the first large-scale assessment of the transcriptome of young and older male and female cell lines and compared them to the muscle transcriptome of their donor. Our sample size was sufficient to identify a distinct transcriptomic signature of age and sex in human muscle tissue, which, except for a few Y-encoded genes, conserved in their corresponding HMPCs. Understanding to what extent sex- and age-specific differences mediated by internal and external factors are retained in culture is essential to establish cause-and-effect relationships between molecular regulators and age- and sex-specific phenotypes before conducting causal validation studies.

Methods

Ethics

This research study was granted ethical approval by the Deakin University Human Research Ethics Committee (DUHREC 2021-307). All participants provided written, informed consent before taking part in the study, which was conducted in accordance with the Declaration of Helsinki (Organisation, 2018) and its later amendments.

Participants

Ten young males (age 18-30), ten young females (age 18-30) and ten older males (age 60-75) were recruited from the local community. These participant cohorts constitute a subset of the broader FaME and MALe studies (DUHREC 2021-307). Inclusion criteria included biologically male and female participants with a normal body mass index (BMI) of 18-35kg/m^2 and deemed generally healthy through completion of a medical questionnaire and assessment by a medical practitioner. Exclusion criteria included type 2 diabetes, a current diagnosis or < 5 years of remission from cancer, a current diagnosis of neurological or neuromuscular disorder, the presence of any infectious bloodborne disease, allergies to anaesthetics, current status as a smoker, the current use of any dietary supplements with the potential to have an effect on muscle metabolism (e.g. thyroxine), any intellectual or mental impairment making it difficult to understand the invasiveness of the medical procedures and provide proper informed consent, and any history of gender affirming treatment of surgery, or hormonal treatment excluding hormonal contraceptives (females only). Participant characteristics are presented in Table 1.

Table 1. Participant characteristics.

Group	**Age**		**Weight**		**Height**		**BMI**	
	Mean	SD	Mean	SD	Mean	SD	Mean	SD
Males (young)	23.22	3.15	76.25	10.94	177.03	7.22	24.26	2.66
Males (older)	67.50	4.19	80.56	13.46	175.04	7.15	26.21	3.26
Females (young)	26.90	6.51	72.33	13.69	165.73	7.92	26.31	4.38

Hormonal status

Female participants were pre-menopausal, not currently pregnant or lactating and completed a menstrual cycle history questionnaire prior to entering the study. Muscle sample collection aimed to occur between day 1-7 of the menstrual cycle, when the ratio of oestrogen to progesterone is the lowest to minimise fluctuations in sex hormones as a potential confounding variable. A blood sample was collected on the same day to control and measures of oestrogen, progesterone, LH and FSH measured by high-performance liquid chromatography mass spectrometry (Triple Quad 5500, Sciex, Framingham, MA) at Monash Health Pathology laboratory (Victoria, Australia) were used to confirm the menstrual status according to (Elliott-Sale et al., 2021).

Muscle sample collection

Participants reported to the laboratory in the morning in a fasted state from 9pm the previous evening. They were provided with a standardized meal of pasta and tomato sauce to eat the night before as previously described (Lamon et al., 2021), and had abstained from caffeine, alcohol, and vigorous physical activity in the 24 hours prior to the visit.

A muscle biopsy was collected from the *vastus lateralis* muscle using the percutaneous needle technique (Bergstrom, 1975) modified to include suction (Shanely et al., 2014) as described in our previous work (Zacharewicz et al., 2014). First, the skin was be sterilised and anaesthetised with 1% Lidocaine without epinephrine. Following this, an incision was made through the skin and fascia and a muscle sample of ~ 100-200 mg was excised. Fifty – 100 mg of muscle was placed in ice-cold serum free Hams F10 nutrient mixture (Thermo Fisher Scientific) for the establishment of primary muscle cell lines. The rest of the sample was immediately snap frozen in liquid isopentane and stored in liquid nitrogen for further analysis.

Human primary cell lines

Thirty individual primary muscle cell lines were established in as previously described in detail by our group in (Zacharewicz et al., 2020). An extra purification step was added when the cells had reached 70-80% confluence, and myogenic satellite cells were purified using Magnetic Activated Cell Sorting (MACS) with anti-

CD56+ microbeads Miltenyi Biotec) as previously described (Agley, Rowlerson, Velloso, Lazarus, & Harridge, 2013; McIlvenna et al., 2021).

Myoblasts were maintained in proliferation media made up of Ham's F-10 medium (Thermo Fisher Scientific) containing 20% FBS, 25 ng/mL fibroblast growth factor (bFGF; Promega), 1% penicillin-streptomycin, and 0.5% amphoteromycin (Life Technologies). At approximately 70–80% confluence, proliferation medium was replaced with differentiation medium made up of DMEM (Life Technologies) containing 5.5mM glucose, 2% HS (New Zealand origin; Gibco, Life Technologies) and 1% penicillin/streptomycin. Differentiation medium was replaced every 48 h. RNA collection was performed on the 9th day of differentiation. The presence of mycoplasma was tested using *contam* (https://github.com/markziemann/contam/tree/main) and revealed an average of 17.8 RPM (range: 8.0 – 22.5 RPM) per sample aligning to one of five antibiotic-resistant mycoplasmic genomes. As a result, the cells were deemed mycoplasma free (Olarerin-George & Hogenesch, 2015).

RNA extraction

RNA was extracted from 10 mg samples of snap frozen *vastus lateralis* tissue or from the pooled content of three technical replicates from 6-well plates, using the AllPrep DNA/RNA/miRNA Universal kit (Qiagen) according to the manufacturer's instructions including proteinase K and DNase treatment. RNA quality and quantity were assessed using the TapeStation System according to manufacturer's instructions (Agilent Technologies). An RNA integrity number (RIN) of >7 was considered acceptable for downstream RNA sequencing analysis.

RNA sequencing, transcript quantification and quality control

The RNAseq libraries were prepared using the Illumina TruSeq Stranded Total RNA with Ribo-Zero Gold protocol and sequenced with 150-bp paired-end reads on the Illumina Novaseq6000 (Macrogen Oceania Platform). Paired-end reads were trimmed of adapters with an average phred score below 10 using Skewer (Jiang, Lei, Ding, & Zhu, 2014). Reads were aligned using Kallisto (Bray et al., 2016) and used to map reads to the reference human transcriptome from Ensembl (genome assembly GRCh38, release-111) and to generate transcript counts. The quality of the

reads before and after trimming and alignment was monitored using FastQC (v0.11.9) (Wingett & Andrews, 2018) and MultiQC (v1.14) (Ewels et al., 2016). The resulting transcriptome count matrix was then mapped to its corresponding gene using biomaRt package (version 2.56.1) (Smedley et al., 2009) and were filtered out of low counts (each gene should contain at least an average of 10 counts across all samples) resulting into 17,789 Ensembl genes IDs for use as input for downstream analysis.

Principal Component Analysis

The filtered count matrix was normalised via the Variance Stabilising Transformation function from the DESeq2 package (v1.40.2) (Love et al., 2014). PCA plots were generated for multiple comparisons using the RNAseqQC package (v0.1.4) (DeLuca et al., 2012).

Differential expression and enrichment analysis

Differential expression (DE) analysis was performed with the DESeq2 package and pipeline using R (v4.3.2) and RStudio (Build 386, "Cherry Blossom" for Ubuntu). A threshold of 0.05 for the Benjamini and Hochberg (BH-adjusted) p values is set as a threshold for significance and a $\log_2$ fold change of 1 and -1 is the threshold set for upregulated and downregulated differentially expressed genes (DEGs) respectively.

Functional enrichment was performed using the GSEA function from the clusterProfiler package (v4.12.6) with Reactome gene sets from the msigdbr package (v7.5.1). The minimum gene set size was set to 10 and a p value cutoff of 0.05. Multidimensional enrichment analysis was conducted using *mitch* (Kaspi & Ziemann, 2020). This package ranks genes by their differential expression based on DESeq2 test statistic before conducting MANOVA based enrichment test. This package generates rank-rank gene density contour heatmaps to depict the similarity between gene expression profiles.

Differentiation time course

A differentiation time course was established on the basis of RNASeq counts from our work (Varshney et al., 2023) deposited on the Gene Expression Ominbus (GEO) platform under accession number GSE168897 and described in (Varshney et al.,

2023). Briefly, one male and one female human skeletal muscle cell line were established according to our existing protocols (Zacharewicz et al., 2020). Myocytes were seeded in 6-well plates and allowed to differentiate as described above. Cell lines were harvested and RNA collected 24hrs after seeding (T1), at the onset of differentiation (T2), as well as after one (T3), three (T4), five (T5) and seven (T6) days of differentiation. Two technical replicates per time point per cell line were analysed.

For initial data preparation, a minimum count threshold of 10 was applied across samples to filter low-expression genes above resulting in 15,859 Ensembl gene IDs. Normalization was conducted through variance-stabilizing transformation (VST), implemented using the *vst* function from DESeq2 (v1.44.0) (Love et al., 2014) ensuring comparable expression data suitable for downstream analysis. Pairwise differential expression analysis was performed across timepoints, and further analysis using the Likelihood Ratio Test in the DESeq2 package was used to identify how genes are differentially expressed between individual timepoints. Genes with similar patterns of expression were clustered using the degPatterns function from the DEGreport package (v1.40.1) (http://lpantano.github.io/DEGreport/).

Differentiation score calculations

Principal component analysis (PCA) was performed on the normalized and transposed count matrix using the *prcomp* function from the *stats* package in R (v4.4.1). The first principal component (PC1) loadings were extracted to capture the most significant variance across genes related to differentiation. Using these PC1 loadings, a weighted sum was computed for each sample, wherein each gene's normalized expression was weighted by its loading in PC1, providing a summary differentiation score per sample based on gene expression. The resulting weighted sums were then min-max scaled, converting values between 0 and 1, enabling consistent comparison across samples and time points. For each sample, the scaled differentiation scores were aggregated by time point, averaging the scores for each time point to represent the differentiation progression over time.

Application of Differentiation Scores to Cell RNASeq Data

To apply the differentiation scores to cell-level data, the normalized cell counts were subset to retain only genes present in the differentiation dataset. The cell differentiation scores were classified into discrete time points by applying threshold values derived from the time-point scores in the differentiation dataset. This classification assigned each cell differentiation score to a specific time point (e.g., T1 through T6), facilitating a temporal interpretation of differentiation states. Scores surpassing the defined thresholds were assigned a classification of "T6_plus" for cells exhibiting differentiation levels beyond the maximum time point threshold.

Results

Differential gene expression in muscle tissue

Forty genes were upregulated, and 46 genes were downregulated in young male when compared to young female muscle tissue (FDR < 0.05, Fig.1A). A Fisher's exact test indicated that the differentially expressed genes were more likely to be encoded by the Y-chromosome (p < 2.2E-16). Among the most downregulated pathways in males according to p-values were several pathways pertaining to cellular respiration and the electron transport chain. The only pathway that was upregulated in males as compared to females was gluconeogenesis (Fig 1B). Fifty-nine genes were upregulated, and 97 genes were downregulated in young male muscle tissue when compared to older male muscle tissue (FDR < 0.05, Fig. 1C). Within the top down-regulated pathways in young males according to p-values were several pathways related to the immune response and the complement cascade. The only pathway that was upregulated in young *versus* older males was antigen processing ubiquitination proteasome degradation (Fig. 1D). Corresponding enrichment score plots can be found in Supplementary Fig. 1A and 1B.

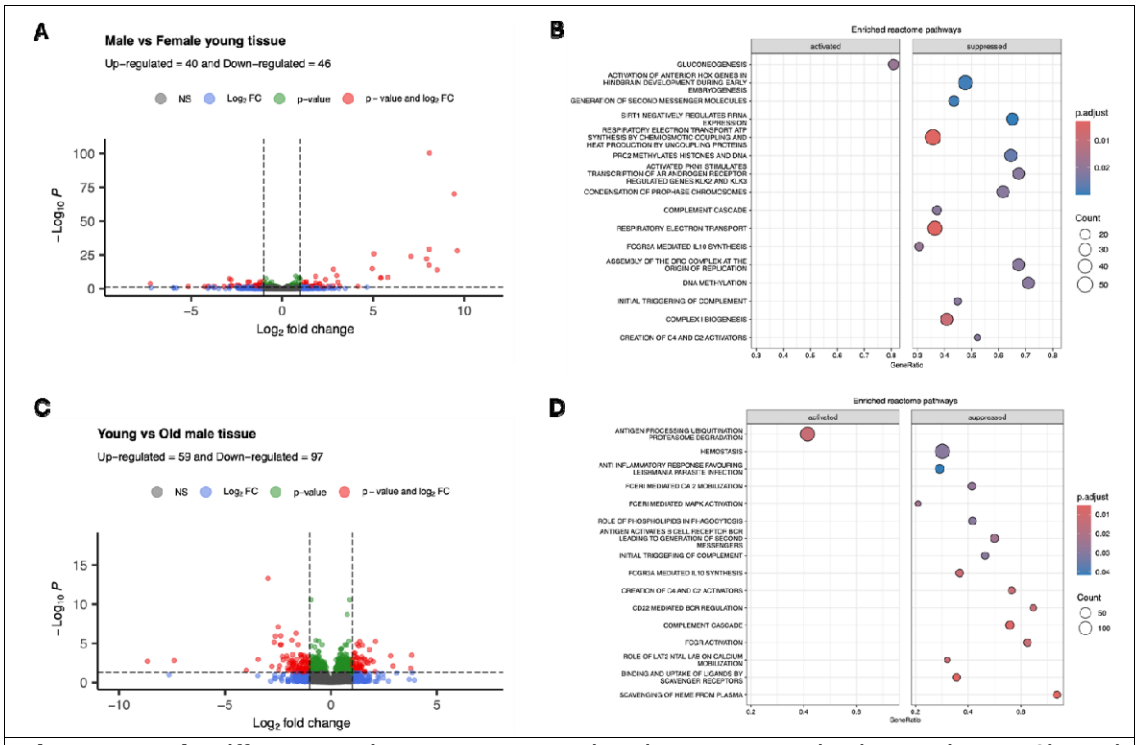

Figure 1. A) Differences in gene expression in young male (control, N=10) and young female (case, N=10) muscle tissue. Genes differentially expressed at FDR

< 0.05 and |Log_2fold change| > 1 are depicted in red. **B)** Reactome pathways upregulated (left panel) or downregulated (right panel) in young male (N=10) versus young female (N=10) muscle tissue. **C)** Differences in gene expression in young male (control, N=10) and older male (case, N=10) muscle tissue. Genes differentially expressed at FDR < 0.05 and |Log_2fold change| > 1 are depicted in red. **D)** Reactome pathways upregulated (left panel) or downregulated (right panel) in young male (N=10) versus older male (N=10) muscle tissue.

Differential gene expression in muscle cell lines

Thirty-two genes were differentially regulated in cell lines grown from young male *versus* young female donors (FDR < 0.05, upregulated: 28, downregulated: 4, Fig. 2A). A Fisher's exact test indicated that the differentially expressed genes were more likely to be encoded by the Y-chromosome (p < 2.2E-16). Similarly, nine genes were differentially regulated in cell lines grown from young *versus* older male donors (FDR < 0.05, upregulated: 3, downregulated: 6, Fig. 2B). In both cases, gene set enrichment analysis (GSEA) resulted in no significantly enriched pathways at the FDR<0.05 significance level.

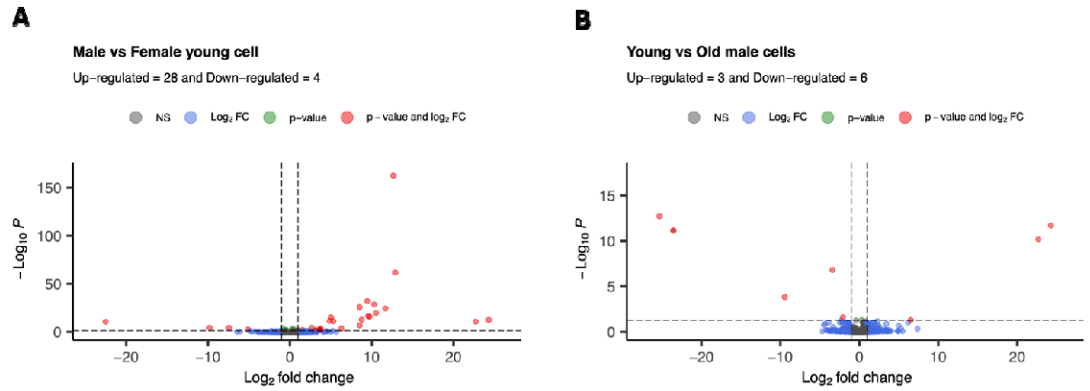

Figure 2. A) Differences in gene expression in HPMC lines grown from young male (control, N = 10) *versus* young female (case, N = 10) donors. **B)** Differences in gene expression in HPMC lines grown from young male (control, N = 10) *versus* older male (case, N = 10) donors. Genes differentially expressed at FDR < 0.05 and |Log_2fold change| > 1 are depicted in red.

Comparison of the transcriptome of muscle tissue and HPMC lines

Differences in the transcriptome of tissue *versus* cell lines were first visualized using principal component analysis (PCA). It revealed a striking separation by sample type (tissue or cells) along the first principal component (88.6%) (Fig. 3A), which was explained by 9595 genes being differentially regulated between muscle tissue and the corresponding HPMC lines (Fig. 3B). Tissue samples formed a tight cluster, while HPMC lines demonstrated a broader spread along the first and second principal component. The main pathways differentially expressed between HPMCs and muscle tissue pertained to energy metabolism (e.g. TCA cycle, respiratory electron transport, mitochondrial biogenesis and complex 1 biogenesis were upregulated in tissue *versus* cells); cell death and senescence (e.g. DNA damage telomere stress induced senescence, diseases of programmed cell death and senescence associated secretory phenotypes SASP were downregulated in tissue *versus* cells); and, interestingly, epigenetic modifications (e.g. DNA methylation, HDACs deacetylate histones and HATS acetylate histones were downregulated in tissue *versus* cells). Corresponding enrichment score plots can be found in Supplementary Fig. 1C.

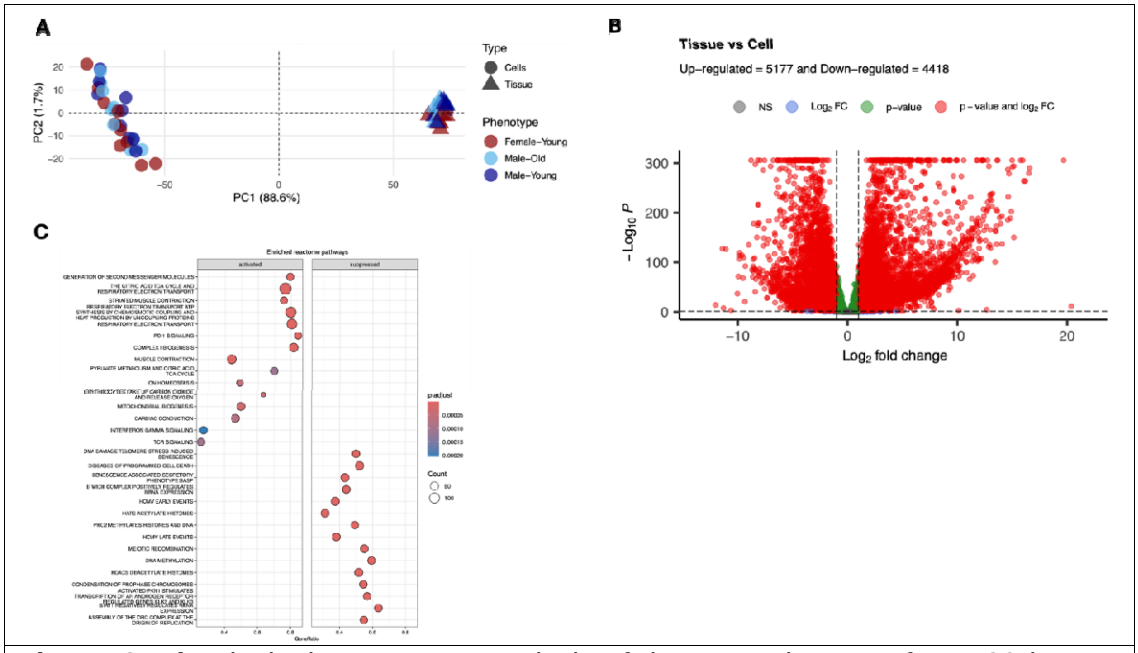

Figure 3. A) Principal component analysis of the transcriptome of N = 30 human muscle tissue samples (control, N = 10 young females, N = 10 young males, N = 10 older males) and the corresponding N = 30 HPMC lines grown from the same donors (case). **B)** Differences in gene expression in human muscle tissue (N=30)

compared to primary muscle cell lines grown from the same donors (N=30). Genes differentially expressed at FDR < 0.05 and |Log_2fold change| > 1 are depicted in red. **C)** Reactome pathways upregulated (left panel) or downregulated (right panel) in muscle tissue (N=30) versus HPMCs (N=30).

Transcriptomic signature of myocyte differentiation

Harvesting thirty cell lines at the same time point inevitably generates some degree of variability in the differentiation level of individual cell lines. Because the degree of satellite cell differentiation into myotubes is complex to assess objectively, we used an existing RNA-seq dataset generated by our group to establish a differentiation signature of human primary myocytes. Rather than relying on a single measure (e.g. fusion index) or a limited number of muscle differentiation markers (e.g. MyoD, MyoG1), we sought to assess the individual level of differentiation of each HPMC line at our experimental endpoint. This was done by comparing its transcriptomic profile to the dynamic signature extracted from an existing, tightly controlled time-course experiment conducted under the same conditions. To define a comprehensive transcriptomic differentiation signature, we first identified genes that were differentially expressed (FDR<0.05) at a given timepoint from the onset of differentiation (T2) comparing each time point to the next (T2 vs T3, T3 vs T4, T4 vs T5, T5 vs T6, Fig. 4A). This analysis resulted in 1411 unique genes (or 8% of all detected genes) that could be grouped in 15 clusters containing 29-773 genes (Fig. 4B). Associated Reactome pathways for the first 10 clusters can be found in Supplementary Fig. 2. The top 3-clusters were respectively enriched in genes related to the cell cycle (cluster 1), lipid metabolism (cluster 2) and muscle contraction (cluster 3).

To establish whether the spread observed along PC1 and PC2 in the cell line cluster (Fig. 3A) could be explained by differences in differentiation between cell lines, we subtracted this list of 1411 genes from the total list of genes and visualized the samples on a PCA plot again. This led to a substantial shift along PC2 (but not PC1) in the spread between individual cell lines and tissue samples (Fig. 4C). More surprisingly, after removing the differentially expressed genes from the PCA analysis, both tissue and cell samples clustered by sex, but not by age, along PC2 (Fig. 4C). In contrast, subtracting a list of 1411 randomly selected genes did not lead to any

visible change (Fig. 4D). This process was repeated 20 times to confirm the spread of the data points remained consistent across the runs.

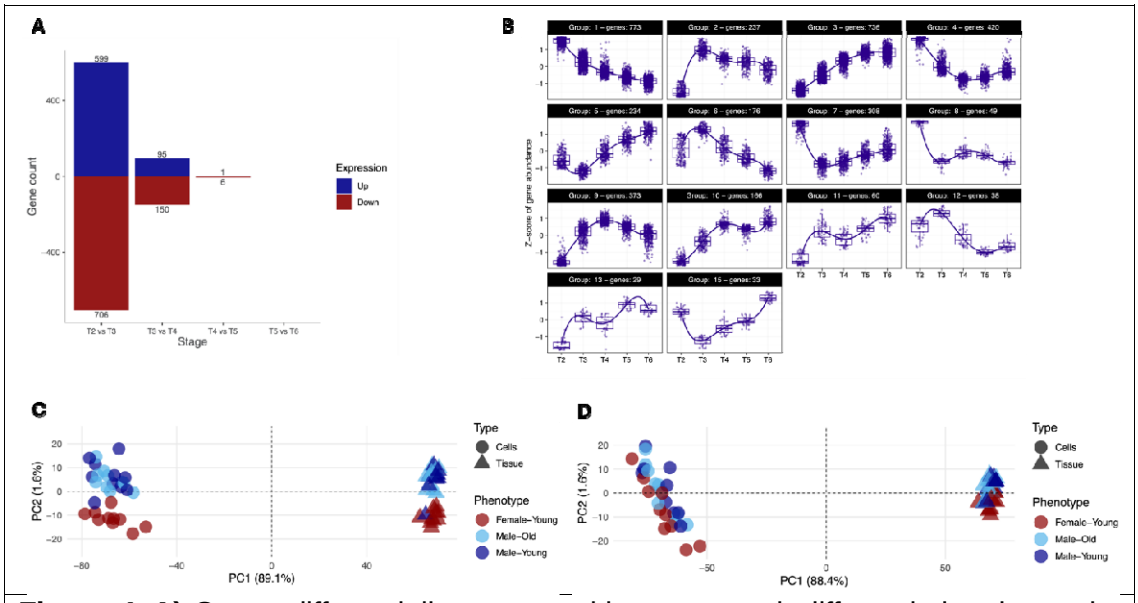

Figure 4. A) Genes differentially expressed between each differentiation time point and the following one (P < 0.05). **B)** Expression profiles of each gene differentially regulated between each differentiation time point and the following one were grouped into 15 clusters containing 29-773 genes. **C)** Principal component analysis of the transcriptome of N = 30 human muscle tissue samples (N = 10 young females, N = 10 young males, N = 10 older females) and the corresponding N = 30 HPMC lines grown from the same donors after 1411 unique genes differentially regulated during differentiation were removed from the analysis. **D)** Principal component analysis of the transcriptome of N = 30 human muscle tissue samples (N = 10 young females, N = 10 young males, N = 10 older females) and the corresponding N = 30 HPMC lines grown from the same donors after 1411 random genes were removed from the analysis.

Differential gene expression in HMPCs when accounting for differentiation score

The transcriptomic profile of our differentiation time course served as a basis to generate a differentiation index comprised between 0-1, where the least differentiated cell lines of the time course were allocated a score closer to 0 and the most differentiated cell lines of the time course were allocated a score closer to 1 (Supplementary Fig. 3). This index was then applied to each HPMC line, which was allocated a differentiation score (Supplementary Table 1) comprised between 0.96 and 1.09 (mean ± SD = 1.03 ± 0.04). To account for the potential influence of the

differentiation status of individual cell lines, differentiation scores were used as a covariate in all further analyses.

Maintenance of the age signature in HPMC lines from male donors

Each individual gene expressed in young and older muscle tissue and in young and older muscle cell lines was plotted on a scatter plot regardless of p-value (Supplementary Fig. 4A). Genes whose differential expression failed to reach statistical significance (FDR < 0.05, log2FC > 1, < -1) between young and older muscle tissue and/or young and older muscle cell lines (represented in yellow in Supplementary Fig. 4A) were then subtracted from the plot (Fig. 5A). Of the remaining genes, only one gene, *HLA-C*, was significantly downregulated in young when compared to older tissue, as well as in young when compared to older cell lines. This was reflected by a Spearman's correlation coefficient of 0.001 from the DESeq2 test statistic of all genes, denoting a lack of association between the two transcriptomic profiles, which can be visualized on the corresponding contour plot (Fig. 5B) that shows genes spread relatively evenly across the four quadrants.

A similar analysis was then repeated at the pathway level. We used *Mitch* to compare the biological pathways that were significantly regulated in the same or in the opposite direction between young and older muscle tissue and/or the corresponding young and older HPMC lines. All significant pathways (p-adjust MANOVA < 0.05) as well as the top-50 significant pathways classified by s-distance (Supplementary Table 2) were visualized on a heatmap (Fig. 5C). Of these, 33 pathways were regulated in the same direction with ageing, and 17 pathways were regulated in the opposite direction with ageing when comparing muscle tissue and HPMC lines. The most strongly differentially regulated pathway was gluconeogenesis, which was enhanced in young versus older tissue but attenuated in young versus older HPMC lines. Other differentially regulated pathways included those involved in cell proliferation, including transcriptional regulation of pluripotent stem cells, FOXO mediated transcription of cell cycle genes and mitotic telophase cytokinesis. All of these pathways were decreased in young versus older tissue but increased in young versus older HPMC lines.

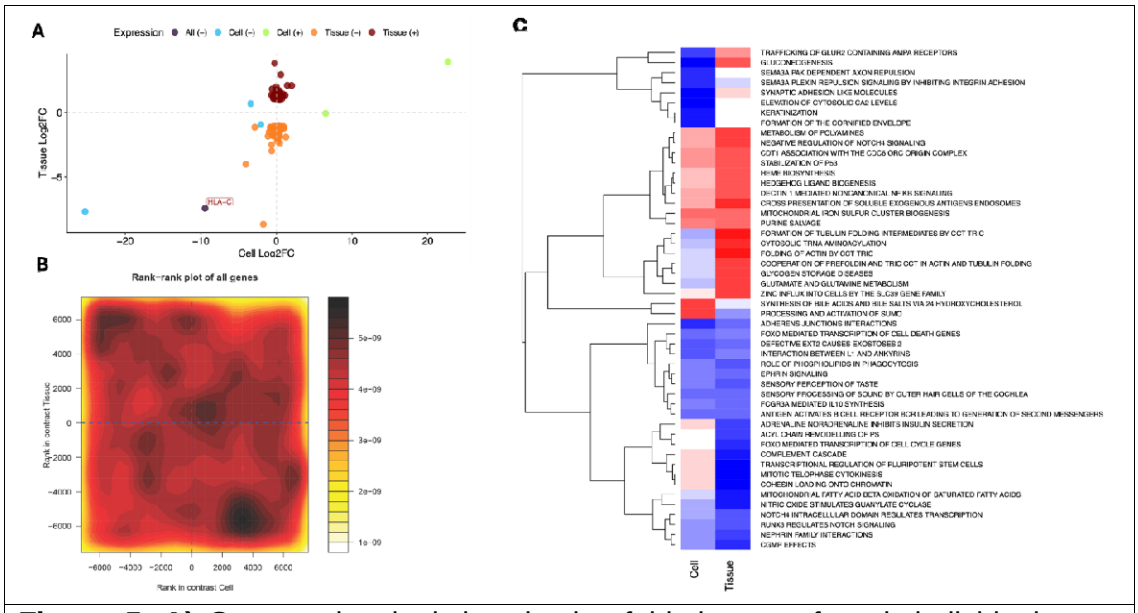

Figure 5. A) Scatter plot depicting the $\log_2$fold-change of each individual gene expressed in young (N=10) and older (N=10) muscle tissue and in the corresponding young (N=10) and older (N=10) muscle cell lines. Genes differentially expressed at FDR < 0.05 and down regulated in both young cell and muscle tissue are depicted in black. Genes differentially expressed at FDR < 0.05 and down regulated in young cell tissue only are depicted in blue. Genes differentially expressed at FDR < 0.05 and up regulated in young cell tissue only are depicted in green. Genes differentially expressed at FDR < 0.05 and down regulated in young muscle tissue only are depicted in orange. Genes differentially expressed at FDR < 0.05 and up regulated in young muscle tissue only are depicted in dark red. **B)** Two-dimensional contour density plot of gene ranks in the cell and age comparisons depicted on the *x* and y axes respectively. **C)** Heatmap depicting the differentially regulated Reactome pathways in young (N=10) and older (N=10) muscle tissue (control) and in the corresponding young (N=10) and older (N=10) HPMC lines (case).

Maintenance of the sex signature in HPMC lines from young donors

Similarly, each gene expressed in young male and female muscle tissue and in young male and female cell lines was plotted on a scatter plot regardless of significance (Supplementary Fig. 4B), including genes encoded on the sex chromosomes. Genes whose differential expression failed to reach statistical significance (FDR < 0.05, log2FC > 1, < -1) between young male and female muscle tissue and/or young male and female muscle cell lines (represented in orange in Supplementary Fig. 4B) were then subtracted from the plot (Fig. 6A). Two genes,

HLC-A and *FEZF2*, were significantly downregulated in male tissue when compared to female tissue, as well as in male HPMC when compared to female HPMC and 11 genes (*TTTY14, PRKY, USP9Y, NLGN4Y, TXLNGY, KDM5D, ZFY, UTY, E1F1AY, DOX3Y, RPS4Y1*) were significantly upregulated in male tissue when compared to female tissue, as well as in male HPMCs when compared to female HPMCs. Spearman's correlation coefficient was -0.06, denoting a weak, negative association of the test statistics between the two transcriptomic profiles, which can be visualized on the corresponding contour plot (Fig. 6B). These figures capture distinct but complementary dimensions of the data, which revealed a positive correlation between the log-fold change of a few genes while some of the remaining genes exhibited a negative association.

A similar analysis was then repeated at the pathway level. All significant pathways (p-adjust MANOVA < 0.05) as well as the top-50 significant pathways classified by s-distance (Supplementary Table 3) were visualized on a heatmap (Fig. 6B). Amongst those, 23 pathways were regulated in the same direction with sex in both tissues and HPMC, and 27 pathways were regulated in opposite directions. For example, gluconeogenesis, the only pathway that was significantly upregulated in male versus female muscle tissue following differential expression analysis, was significantly downregulated in male versus female HPMCs.

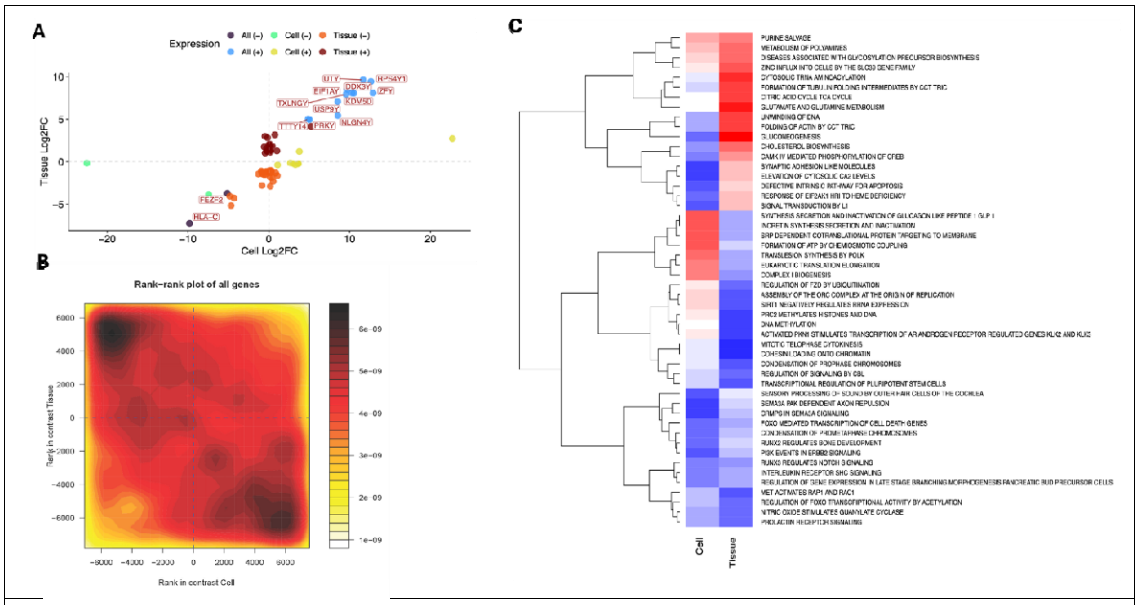

Figure 6. Scatter plots depicting the $\log_2$fold-change of each individual gene expressed in young male (N=10) and young female (N=10) muscle tissue and in the corresponding young male (N=10) and young female (N=10) muscle cell lines.

Genes differentially expressed at FDR < 0.05 and down regulated in both female cell and muscle tissue are depicted in black. Genes differentially expressed at FDR < 0.05 and upregulated in both male cell and male muscle tissue are depicted in blue. Genes differentially expressed at FDR < 0.05 and down regulated in male cells only are depicted in aqua. Genes differentially expressed at FDR < 0.05 and down regulated in male muscle tissue only are depicted in dark orange. Genes differentially expressed at FDR < 0.05 and up regulated in male muscle tissue only are depicted in dark red. **B)** Differential expression rank-rank density contour plot with cell and tissue contrasts on the x and y axes. **C)** Heatmap depicting the differentially regulated pathways in young male (N=10) and female (N=10) muscle tissue (control) and in the corresponding young male (N=10) and female (N=10) muscle cell lines (case).

Discussion

First isolated in 1981 (Blau & Webster, 1981), HPMCs constitute a common experimental model in muscle research due to the relative ease of access to human skeletal muscle tissue using well-established percutaneous biopsy techniques (Bergstrom, 1975). Despite their intrinsic genetic heterogeneity, HPMCs are often preferred to the commercially available mouse C_2C_{12} or rat H6 muscle cell lines due to their non-immortalized nature and perceived closeness to a human physiological system. Indeed, there are important transcriptional and metabolic differences between HPMCs, C_2C_{12} and H6 myocytes (Abdelmoez et al., 2020). However, the variability between the transcriptome of muscle tissue and cultured myocytes from the same species (human, mouse or rat) is larger than the variability between the muscle tissue transcriptomes from different species, or between cultured myocytes transcriptomes from different species (Abdelmoez et al., 2020). An extension of the premise that HPMCs accurately mimic a human physiological system is the common use of HPMC lines that share traits with the population of interest (e.g. “aged” muscle cell lines, “female” muscle cell lines) to probe age- or sex-specific mechanisms. The assumption underlying such practise is that HPMCs retain some key phenotypical characteristics from their donors once placed in culture despite the removal of the systemic environment. Here we directly tested this assumption by conducting an in-depth comparison of the transcriptome of young male, young female, and older male muscle tissue to their corresponding HPMCs at the individual gene and pathway level.

As expected, we found differences between the transcriptome of young male versus female muscle tissue (Oliva et al., 2020), as well as between young versus older male muscle tissue (de Jong et al., 2023; Gharpure et al., 2023; Schaiter et al., 2024; Tumasian et al., 2021). The discovery of sex-specific differences during the ageing process was beyond the scope of this study. Generally, these differences did not translate to the corresponding HPMC lines. Thirty-two individual genes were differentially regulated in HPMCs grown from young male versus young female donors (replicating the micro-array based findings from (Davegårdh et al., 2019)) and nine individual genes were differentially regulated in HPMCs grown from young versus older male donors, respectively. Regarding the maintenance of the age phenotype, only one gene (*HLA-C*) remained differentially regulated in the same

direction in both tissue and HPMCs (Spearman's correlation coefficient = 0.001). Regarding the maintenance of the sex phenotype, 13 genes (*TTTY14, PRKY, USP9Y, NLGN4Y, TXLNGY, 4DM50, ZFY, UTY, E1F1AY, DOX3Y, RPS4Y1, FEZF2, HLA-C*) remained differentially regulated in the same direction in both tissue and HPMCs, despite a negative Spearman's correlation coefficient (-0.06). This strongly suggests that the expression of some other significantly regulated genes, which were not specifically investigated in this study, must have exhibited a reversed association between tissue and their corresponding HPMCs; a hypothesis supported by our pathway analysis.

HLA-C, the only gene whose differential expression was maintained with age, encodes a protein belonging to the major histocompatibility complex (MHC) class I family and was significantly downregulated in young versus older samples in both tissue and cells (> 5-fold in tissue, > 10-fold in HPMCs). An altered immune response (also termed "immunosenescence") is both a consequence and an indirect hallmark of ageing (López-Otín et al., 2013), including at the transcriptomic level (Tumasian et al., 2021). Ageing is however also characterized by a constitutive, low-level activation of the immune system (Shaw et al., 2010), which may explain that some immune features increase rather than decrease with age. Pathway analysis offers higher-level insights into the maintenance of the muscle immune phenotype with ageing in tissue and HPMCs. While HLC-A was regulated in the same direction in tissue and HPMCs, the complement cascade, for example, was downregulated in young versus older tissue, but upregulated in young versus older HPMCs. These disparities may be due to the fact that whole skeletal muscle tissue inevitably contains resident immune cells (Pillon et al., 2013), including T-cells and at least two populations of macrophages (Jensen et al., 2021). These cells are filtered out by the muscle specific anti-CD56+ antibodies used in the process of establishing cultured myocytes, which may influence individual gene expression across certain cellular pathways such as those related to immunity. However, other striking contrasts that could not be directly attributed to differences in cell populations were also evident in the cellular pathways pertaining to the regulation of the cell cycle (e.g. FOXO-mediated regulation of cell cycle genes, transcriptional regulation of pluripotent stem cell and mitotic telophase cytokinesis decreased in young versus older tissue but increased in the corresponding HPMCs) or substrate metabolism (e.g.

gluconeogenesis, glycogen storage diseases and glutamine/glutamate metabolism increased in young versus older tissue but decreased in the corresponding HPMCs).

All 11 genes that remained up-regulated in both male versus female tissue and cells were Y-encoded. Of the two genes that remained down-regulated in both male versus female tissue and cells, FEZF2 is a sexually dimorphic protein-coding gene encoding a transcription factor important to cell fate in the development of the nervous system in mammals (Eckler & Chen, 2014; Lodato et al., 2014). In turtle gonads, which are subjected to temperature-dependent sex-determination, FEZF2 is hypermethylated in females versus males (Radhakrishnan et al., 2017), suggesting a role in sexual differentiation, but how this may translate to other tissues and species remains unknown.

These wide transcriptomic differences between human muscle tissue and their corresponding HMPCs may be explained in two ways. Firstly, in mammals, skeletal muscle fibres make up to 95% of the volume of muscle tissue but display relatively sparse nuclei when compared to their cell size. In addition, whole muscle biopsies not only contain myoblasts and mature muscle cells, but also fibro-adipogenic progenitors, immune cells, fibroblasts and endothelial cells (Jensen et al., 2021; Pillon et al., 2013). The ratio of muscle nuclei may in fact be as little as 50% (Bruusgaard & Gundersen, 2008; Schmalbruch & Hellhammer, 1977) and, while myocytes remain the most transcriptionally active cell type in the muscle (Kirby et al., 2016), these aspects must be considered when comparing patterns of gene expression between whole muscle tissue and cultured muscle cells that have been subjected to muscle-specific cell selection. Secondly, the hormonal environment drastically varies between young males and females, exerting a sex-specific effect on numerous tissues including skeletal muscle (reviewed in (Landen et al., 2021)). Circulating concentrations of androgenic and oestrogenic hormones are highly sex specific. In addition, these hormones enact their effects through specific receptors that can be differentially regulated with sex (Vingren et al., 2009) or show sex-biased activation patterns (Lopes-Ramos et al., 2020). Our results indicate that the removal of the sex-determining hormonal milieu is enough to conceal most transcriptomic differences due to sex *in vitro*, including some of the differences mediated by the Y chromosome complement independent of sex hormones (Arnold, 2017; Wijchers et al., 2010). The same may be true, to an extent, with the ageing process. In males,

ageing is associated with profound declines in androgen concentrations, particularly testosterone (Chu et al., 2008; Liu et al., 2015). The direct effects of testosterone on age-related molecular mechanisms in the muscle are yet to be determined, especially *in vivo*, but evidence suggests that testosterone decline impacts several pathways important to the maintenance of skeletal muscle cells with ageing. These include muscle fibre hypertrophy through the suppression of ubiquitin-ligase mediated atrophic pathways, or satellite cell proliferation through the synthesis of cell-cycle regulating proteins such as follistatin and Notch receptors (Braga et al., 2012; Rana et al., 2014). Prior research in C_2C_{12} has mimicked aspects of ageing in cells, where subjecting the cells to multiple-population-doubling resulted in impaired myoblast fusion and upregulated myostatin and TNF-α (Sharples et al., 2012); effects that could be partially rescued by testosterone treatment (Deane et al., 2013; Hughes et al., 2016). Multiple-population-doubling is however not applicable to HPMCs, and the lack of androgens and other growth factors in the cellular milieu suggests a major role for these hormones in the determination of the ageing muscle phenotype. Conversely, the presence of foetal growth factors in the proliferation medium may push the cells towards a “younger” phenotype.

An intriguing finding was the observation that removing a group of 1411 unique genes from our principal component analysis led to a clear differentiation by sex, but not age. These genes were those whose individual expression significantly varied at one stage of HPMC differentiation or more. This finding indicates that differences due to fundamental biological factors (here: sex) were previously masked by the variability resulting from the differential expression of this group of genes. This variability, however, could not be attributed to differences in differentiation itself, which was minimal in our terminally differentiated HPMC lines, as indicated by our differentiation scores, and should be irrelevant in healthy (i.e. non-injured) human muscle collected from a homogenous age group. The main genes fluctuating during muscle cell proliferation and differentiation (e.g. PAX3, PAX7, MYOD, MYOG, MYF5, MYF6) somehow recapitulate the gene expression pattern observed in post-natal mammalian muscle development (Lamon et al., 2017) and regeneration (Mikovic et al., 2020). Our results suggest that, collectively, the influence of the individual level of expression of these genes in terminally differentiated human muscle fibres or

HPMCs is still important enough to conceal fundamental differences due to sex -, but not to age.

In conclusion, we provide evidence that the transcriptomic signature of sex (Spearman's correlation coefficient = -0.06) and age (Spearman's correlation coefficient = 0.001) in human muscle tissue is mostly lost once cultured *in vitro*. At the individual gene level, this loss of phenotype is as prominent for age as it is for sex, despite the maintained differential expression of Y-linked genes, whose sex-specific expression was significantly more likely to remain conserved in both tissue and cell lines. The transcriptome only provides insights into one layer of metabolic and functional regulation though, and these results should be further validated, for example at the proteomics, phenotypic and function levels, before discounting the use of HMPCs as age- or sex-specific models of human skeletal muscle. Our findings also do not exclude the possibility that some sex- or age-specific phenotypes might be lost at baseline but become apparent in response to an external stimulus (e.g. hormone treatment, electrostimulation, miRNA transfection) as previously shown by our group (Hiam et al., 2023). It is also possible that cell culture media may be supplemented with specific age- and sex-specific circulating growth factors to achieve a model transcriptionally closer to the source phenotype. Finally, nuclear single cell sequencing or HMPCs grown in 3D culture as organoids under strain might provide a closer comparison between human muscle fibres and their corresponding HPMCs. Our results generally call for caution, and any claim that HPMCs can be used as an experimental model of human muscle sex or age should be interpreted carefully.

Acknowledgements

The authors would like to acknowledge Dr Sarah Voisin (Novo Nordisk) for her precious advice. Funding: This research was supported by use of the Nectar Research Cloud, a collaborative Australian research platform supported by the NCRIS-funded Australian Research Data Commons (ARDC). The authors gratefully acknowledge the contribution to this work of the Victorian Operational Infrastructure Support Program received by the Burnet Institute. Séverine Lamon and this study were supported by an Australian Research Council Future Fellowship (FT10100278).

Conflict of Interest statement

The authors have no conflict of interest to declare.

Authors' contributions

SL designed the study, analysed the data, interpreted the data and funded the study. MS analysed the data and interpreted the data. RW, AC and AG collected the samples and generated the data. AV and TB generated and analysed the differentiation data. DH collected the samples, analysed the data and interpreted the data. MZ designed the study and interpreted the data. All authors contributed to the preparation of the manuscript.

Data availability statement

All transcriptomic data are deposited in an online repository and are available upon request. The full code is available at https://github.com/megan-soria/age_and_sex_signature. The *contam* package is available at https://github.com/markziemann/contam/tree/main.

References

Abdelmoez, A. M., Sardón Puig, L., Smith, J. A. B., Gabriel, B. M., Savikj, M., Dollet, L., . . . Pillon, N. J. (2020). Comparative profiling of skeletal muscle models reveals heterogeneity of transcriptome and metabolism. *Am J Physiol Cell Physiol, 318*(3), C615-c626. doi:10.1152/ajpcell.00540.2019

Agley, C. C., Rowlerson, A. M., Velloso, C. P., Lazarus, N. R., & Harridge, S. D. R. (2013). Human skeletal muscle fibroblasts, but not myogenic cells, readily undergo adipogenic differentiation. *Journal of Cell Science, 126*(24), 5610-5625. doi:10.1242/jcs.132563

Alsharidah, M., Lazarus, N. R., George, T. E., Agley, C. C., Velloso, C. P., & Harridge, S. D. (2013). Primary human muscle precursor cells obtained from young and old donors produce similar proliferative, differentiation and senescent profiles in culture. *Aging Cell, 12*(3), 333-344. doi:10.1111/acel.12051

Arentson-Lantz, E. J., Fiebig, K. N., Anderson-Catania, K. J., Deer, R. R., Wacher, A., Fry, C. S., . . . Paddon-Jones, D. (2020). Countering disuse atrophy in older adults with low-volume leucine supplementation. *J Appl Physiol (1985), 128*(4), 967-977. doi:10.1152/japplphysiol.00847.2019

Arentson-Lantz, E. J., Mikovic, J., Bhattarai, N., Fry, C. S., Lamon, S., Porter, C., & Paddon-Jones, D. (2021). Leucine augments specific skeletal muscle mitochondrial respiratory pathways during recovery following 7 days of physical inactivity in older adults. *J Appl Physiol (1985), 130*(5), 1522-1533. doi:10.1152/japplphysiol.00810.2020

Arnold, A. P. (2017). A general theory of sexual differentiation. *J Neurosci Res, 95*(1-2), 291-300. doi:10.1002/jnr.23884

Bergstrom, J. (1975). Percutaneous needle biopsy of skeletal muscle in physiological and clinical research. *Scand J Clin Lab Invest, 35*(7), 609-616. Retrieved from https://www.ncbi.nlm.nih.gov/pubmed/1108172

Blau, H. M., & Webster, C. (1981). Isolation and characterization of human muscle cells. *Proc Natl Acad Sci U S A, 78*(9), 5623-5627. doi:10.1073/pnas.78.9.5623

Braga, M., Bhasin, S., Jasuja, R., Pervin, S., & Singh, R. (2012). Testosterone inhibits transforming growth factor-β signaling during myogenic differentiation and proliferation of mouse satellite cells: potential role of follistatin in mediating testosterone action. *Mol Cell Endocrinol, 350*(1), 39-52. doi:10.1016/j.mce.2011.11.019

Bray, N. L., Pimentel, H., Melsted, P., & Pachter, L. (2016). Near-optimal probabilistic RNA-seq quantification. *Nat Biotechnol, 34*(5), 525-527. doi:10.1038/nbt.3519

Bruusgaard, J. C., & Gundersen, K. (2008). In vivo time-lapse microscopy reveals no loss of murine myonuclei during weeks of muscle atrophy. *J Clin Invest, 118*(4), 1450-1457. doi:10.1172/jci34022

Burattini, S., Ferri, P., Battistelli, M., Curci, R., Luchetti, F., & Falcieri, E. (2004). C2C12 murine myoblasts as a model of skeletal muscle development: morpho-functional characterization. *Eur J Histochem, 48*(3), 223-233.

Chu, L.-W., Tam, S., Kung, A. W. C., Lo, S., Fan, S., Wong, R. L. C., . . . Lam, K. S. L. (2008). Serum Total and Bioavailable Testosterone Levels, Central Obesity, and Muscle Strength Changes with Aging in Healthy Chinese Men. *Journal of the American Geriatrics Society, 56*(7), 1286-1291. doi:https://doi.org/10.1111/j.1532-5415.2008.01746.x

Conboy, I. M., Conboy, M. J., Wagers, A. J., Girma, E. R., Weissman, I. L., & Rando, T. A. (2005). Rejuvenation of aged progenitor cells by exposure to a young systemic environment. *Nature, 433*(7027), 760-764. doi:10.1038/nature03260

Davegårdh, C., Hall Wedin, E., Broholm, C., Henriksen, T. I., Pedersen, M., Pedersen, B. K., . . . Ling, C. (2019). Sex influences DNA methylation and gene expression in human skeletal muscle myoblasts and myotubes. *Stem Cell Research & Therapy, 10*(1), 26. doi:10.1186/s13287-018-1118-4

de Jong, J., Attema, B. J., van der Hoek, M. D., Verschuren, L., Caspers, M. P. M., Kleemann, R., . . . Keijer, J. (2023). Sex differences in skeletal muscle-aging trajectory: same processes, but with a different ranking. *Geroscience, 45*(4), 2367-2386. doi:10.1007/s11357-023-00750-4

Deane, C. S., Hughes, D. C., Sculthorpe, N., Lewis, M. P., Stewart, C. E., & Sharples, A. P. (2013). Impaired hypertrophy in myoblasts is improved with testosterone administration. *J Steroid Biochem Mol Biol, 138*, 152-161. doi:10.1016/j.jsbmb.2013.05.005

Deasy, B. M., Lu, A., Tebbets, J. C., Feduska, J. M., Schugar, R. C., Pollett, J. B., . . . Huard, J. (2007). A role for cell sex in stem cell-mediated skeletal muscle regeneration: female cells have higher muscle regeneration efficiency. *J Cell Biol, 177*(1), 73-86. doi:10.1083/jcb.200612094

DeLuca, D. S., Levin, J. Z., Sivachenko, A., Fennell, T., Nazaire, M. D., Williams, C., . . . Getz, G. (2012). RNA-SeQC: RNA-seq metrics for quality control and process optimization. *Bioinformatics, 28*(11), 1530-1532. doi:10.1093/bioinformatics/bts196

Eckler, M. J., & Chen, B. (2014). Fez family transcription factors: controlling neurogenesis and cell fate in the developing mammalian nervous system. *Bioessays, 36*(8), 788-797. doi:10.1002/bies.201400039

Elliott-Sale, K. J., Minahan, C. L., de Jonge, X., Ackerman, K. E., Sipilä, S., Constantini, N. W., . . . Hackney, A. C. (2021). Methodological Considerations for Studies in Sport and Exercise Science with Women as Participants: A Working Guide for Standards of Practice for Research on Women. *Sports Med, 51*(5), 843-861. doi:10.1007/s40279-021-01435-8

English, K. L., & Paddon-Jones, D. (2010). Protecting muscle mass and function in older adults during bed rest. *Curr Opin Clin Nutr Metab Care, 13*(1), 34-39. doi:10.1097/MCO.0b013e328333aa66

Ewels, P., Magnusson, M., Lundin, S., & Kaller, M. (2016). MultiQC: summarize analysis results for multiple tools and samples in a single report. *Bioinformatics, 32*(19), 3047-3048. doi:10.1093/bioinformatics/btw354

Gharpure, M., Chen, J., Nerella, R., Vyavahare, S., Kumar, S., Isales, C. M., . . . Fulzele, S. (2023). Sex-specific alteration in human muscle transcriptome with age. *Geroscience, 45*(3), 1303-1316. doi:10.1007/s11357-023-00795-5

Haizlip, K. M., Harrison, B. C., & Leinwand, L. A. (2015). Sex-based differences in skeletal muscle kinetics and fiber-type composition. *Physiology (Bethesda), 30*(1), 30-39. doi:10.1152/physiol.00024.2014

Hiam, D., Landen, S., Jacques, M., Voisin, S., Lamon, S., & Eynon, N. (2023). Muscle miRNAs are influenced by sex at baseline and in response to exercise. *BMC Biol, 21*(1), 273. doi:10.1186/s12915-023-01755-3

Hughes, D. C., Stewart, C. E., Sculthorpe, N., Dugdale, H. F., Yousefian, F., Lewis, M. P., & Sharples, A. P. (2016). Testosterone enables growth and hypertrophy in fusion impaired myoblasts that display myotube atrophy: deciphering the

role of androgen and IGF-I receptors. *Biogerontology, 17*(3), 619-639. doi:10.1007/s10522-015-9621-9

Jensen, J. B., Møller, A. B., Just, J., Mose, M., de Paoli, F. V., Billeskov, T. B., . . . Jessen, N. (2021). Isolation and characterization of muscle stem cells, fibro-adipogenic progenitors, and macrophages from human skeletal muscle biopsies. *American Journal of Physiology-Cell Physiology, 321*(2), C257-C268. doi:10.1152/ajpcell.00127.2021

Jiang, H., Lei, R., Ding, S. W., & Zhu, S. (2014). Skewer: a fast and accurate adapter trimmer for next-generation sequencing paired-end reads. *BMC Bioinformatics, 15*, 182. doi:10.1186/1471-2105-15-182

Kase, E. T., Feng, Y. Z., Badin, P. M., Bakke, S. S., Laurens, C., Coue, M., . . . Moro, C. (2015). Primary defects in lipolysis and insulin action in skeletal muscle cells from type 2 diabetic individuals. *Biochim Biophys Acta, 1851*(9), 1194-1201. doi:10.1016/j.bbalip.2015.03.005

Kaspi, A., & Ziemann, M. (2020). mitch: multi-contrast pathway enrichment for multi-omics and single-cell profiling data. *BMC Genomics, 21*(1), 447. doi:10.1186/s12864-020-06856-9

Kirby, T. J., Patel, R. M., McClintock, T. S., Dupont-Versteegden, E. E., Peterson, C. A., & McCarthy, J. J. (2016). Myonuclear transcription is responsive to mechanical load and DNA content but uncoupled from cell size during hypertrophy. *Mol Biol Cell, 27*(5), 788-798. doi:10.1091/mbc.E15-08-0585

Lamon, S., Morabito, A., Arentson-Lantz, E., Knowles, O., Vincent, G. E., Condo, D., . . . Aisbett, B. (2021). The effect of acute sleep deprivation on skeletal muscle protein synthesis and the hormonal environment. *Physiological Reports, 9*(1), e14660-e14660. doi:10.14814/phy2.14660

Lamon, S., Zacharewicz, E., Arentson-Lantz, E., Gatta, P. A., Ghobrial, L., Gerlinger-Romero, F., . . . Russell, A. P. (2016). Erythropoietin Does Not Enhance Skeletal Muscle Protein Synthesis Following Exercise in Young and Older Adults. *Front Physiol, 7*, 292. doi:10.3389/fphys.2016.00292

Lamon, S., Zacharewicz, E., Butchart, L. C., Orellana, L., Mikovic, J., Grounds, M. D., & Russell, A. P. (2017). MicroRNA expression patterns in post-natal mouse skeletal muscle development. *BMC Genomics, 18*(1), 52. doi:10.1186/s12864-016-3399-2

Landen, S., Hiam, D., Voisin, S., Jacques, M., Lamon, S., & Eynon, N. (2021). Physiological and molecular sex differences in human skeletal muscle in response to exercise training. *J Physiol*. doi:10.1113/jp279499

Lee, C., Woods, P. C., Paluch, A. E., & Miller, M. S. (2024). Effects of age on human skeletal muscle: A systematic review and meta-analysis of myosin heavy chain isoform protein expression, fiber size and distribution. *Am J Physiol Cell Physiol*. doi:10.1152/ajpcell.00347.2024

Liu, Z., Liu, J., Shi, X., Wang, L., Yang, Y., & Tao, M. (2015). Dynamic alteration of serum testosterone with aging: a cross-sectional study from Shanghai, China. *Reproductive Biology and Endocrinology, 13*(1). doi:10.1186/s12958-015-0107-z

Lodato, S., Molyneaux, B. J., Zuccaro, E., Goff, L. A., Chen, H.-H., Yuan, W., . . . Arlotta, P. (2014). Gene co-regulation by Fezf2 selects neurotransmitter identity and connectivity of corticospinal neurons. *Nature Neuroscience, 17*(8), 1046-1054. doi:10.1038/nn.3757

Lopes-Ramos, C. M., Chen, C. Y., Kuijjer, M. L., Paulson, J. N., Sonawane, A. R., Fagny, M., . . . DeMeo, D. L. (2020). Sex Differences in Gene Expression and

Regulatory Networks across 29 Human Tissues. *Cell Rep, 31*(12), 107795. doi:10.1016/j.celrep.2020.107795
López-Otín, C., Blasco, M. A., Partridge, L., Serrano, M., & Kroemer, G. (2013). The hallmarks of aging. *Cell, 153*(6), 1194-1217. doi:10.1016/j.cell.2013.05.039
Love, M. I., Huber, W., & Anders, S. (2014). Moderated estimation of fold change and dispersion for RNA-seq data with DESeq2. *Genome Biol, 15*(12), 550. doi:10.1186/s13059-014-0550-8
McIlvenna, L. C., Patten, R. K., McAinch, A. J., Rodgers, R. J., Stepto, N. K., & Moreno-Asso, A. (2021). Transforming Growth Factor Beta 1 Alters Glucose Uptake but Not Insulin Signalling in Human Primary Myotubes From Women With and Without Polycystic Ovary Syndrome. *Frontiers in Endocrinology, 12*. doi:10.3389/fendo.2021.732338
Mikovic, J., Brightwell, C., Lindsay, A., Wen, Y., Kowalski, G., Russell, A. P., . . . Lamon, S. (2020). An obesogenic maternal environment impairs mouse growth patterns, satellite cell activation, and markers of postnatal myogenesis. *Am J Physiol Endocrinol Metab, 319*(6), E1008-e1018. doi:10.1152/ajpendo.00398.2020
Olarerin-George, A. O., & Hogenesch, J. B. (2015). Assessing the prevalence of mycoplasma contamination in cell culture via a survey of NCBI's RNA-seq archive. *Nucleic Acids Research, 43*(5), 2535-2542. doi:10.1093/nar/gkv136
Oliva, M., Munoz-Aguirre, M., Kim-Hellmuth, S., Wucher, V., Gewirtz, A. D. H., Cotter, D. J., . . . Stranger, B. E. (2020). The impact of sex on gene expression across human tissues. *Science, 369*(6509). doi:10.1126/science.aba3066
Organisation, W. M. (2018). *WMA Declaration of Helsinki - Ethical principles for medical research involvoing human subjects*. Retrieved from https://www.wma.net/policies-post/wma-declaration-of-helsinki-ethical-principles-for-medical-research-involving-human-subjects/
Pillon, N. J., Bilan, P. J., Fink, L. N., & Klip, A. (2013). Cross-talk between skeletal muscle and immune cells: muscle-derived mediators and metabolic implications. *American Journal of Physiology-Endocrinology and Metabolism, 304*(5), E453-E465. doi:10.1152/ajpendo.00553.2012
Radhakrishnan, S., Literman, R., Mizoguchi, B., & Valenzuela, N. (2017). MeDIP-seq and nCpG analyses illuminate sexually dimorphic methylation of gonadal development genes with high historic methylation in turtle hatchlings with temperature-dependent sex determination. *Epigenetics Chromatin, 10*, 28. doi:10.1186/s13072-017-0136-2
Rana, K., Lee, N. K., Zajac, J. D., & MacLean, H. E. (2014). Expression of androgen receptor target genes in skeletal muscle. *Asian J Androl, 16*(5), 675-683. doi:10.4103/1008-682x.122861
Schaiter, A., Hentschel, A., Kleefeld, F., Schuld, J., Umathum, V., Procida-Kowalski, T., . . . Schanzer, A. (2024). Molecular composition of skeletal muscle in infants and adults: a comparative proteomic and transcriptomic study. *Sci Rep, 14*(1), 22965. doi:10.1038/s41598-024-74913-4
Schmalbruch, H., & Hellhammer, U. (1977). The number of nuclei in adult rat muscles with special reference to satellite cells. *Anat Rec, 189*(2), 169-175. doi:10.1002/ar.1091890204
Seale, K., Horvath, S., Teschendorff, A., Eynon, N., & Voisin, S. (2022). Making sense of the ageing methylome. *Nat Rev Genet, 23*(10), 585-605. doi:10.1038/s41576-022-00477-6

Shanely, R. A., Zwetsloot, K. A., Triplett, N. T., Meaney, M. P., Farris, G. E., & Nieman, D. C. (2014). Human Skeletal Muscle Biopsy Procedures Using the Modified Bergström Technique. *Journal of Visualized Experiments*(91). doi:10.3791/51812

Sharples, A. P., Player, D. J., Martin, N. R. W., Mudera, V., Stewart, C. E., & Lewis, M. P. (2012). Modelling*in vivo*skeletal muscle ageing*in vitro*using three-dimensional bioengineered constructs. *Aging Cell, 11*(6), 986-995. doi:10.1111/j.1474-9726.2012.00869.x

Shaw, A. C., Joshi, S., Greenwood, H., Panda, A., & Lord, J. M. (2010). Aging of the innate immune system. *Curr Opin Immunol, 22*(4), 507-513. doi:10.1016/j.coi.2010.05.003

Smedley, D., Haider, S., Ballester, B., Holland, R., London, D., Thorisson, G., & Kasprzyk, A. (2009). BioMart--biological queries made easy. *BMC Genomics, 10*, 22. doi:10.1186/1471-2164-10-22

Tieland, M., Trouwborst, I., & Clark, B. C. (2018). Skeletal muscle performance and ageing. *J Cachexia Sarcopenia Muscle, 9*(1), 3-19. doi:10.1002/jcsm.12238

Tumasian, R. A., Harish, A., Kundu, G., Yang, J.-H., Ubaida-Mohien, C., Gonzalez-Freire, M., . . . Ferrucci, L. (2021). Skeletal muscle transcriptome in healthy aging. *Nature Communications, 12*(1), 2014. doi:10.1038/s41467-021-22168-2

Turner, D. C., Gorski, P. P., Maasar, M. F., Seaborne, R. A., Baumert, P., Brown, A. D., . . . Sharples, A. P. (2020). DNA methylation across the genome in aged human skeletal muscle tissue and muscle-derived cells: the role of HOX genes and physical activity. *Sci Rep, 10*(1), 15360. doi:10.1038/s41598-020-72730-z

Varshney, A. H., P.F.;Swaminathan, A.; Alexander, S.E.; Dichtl, B.;Lamon, S.;Beilharz, T.H. (2023). *Primary human myoblasts display only minor alternative polyadenylation compared to the transformed C2C12 model of muscle differentiation*. Retrieved from https://www.biorxiv.org/content/10.1101/2023.12.17.572066v1

Vingren, J. L., Kraemer, W. J., Hatfield, D. L., Volek, J. S., Ratamess, N. A., Anderson, J. M., . . . Maresh, C. M. (2009). Effect of resistance exercise on muscle steroid receptor protein content in strength-trained men and women. *Steroids, 74*(13-14), 1033-1039. doi:10.1016/j.steroids.2009.08.002

Wijchers, P. J., Yandim, C., Panousopoulou, E., Ahmad, M., Harker, N., Saveliev, A., . . . Festenstein, R. (2010). Sexual Dimorphism in Mammalian Autosomal Gene Regulation Is Determined Not Only by Sry but by Sex Chromosome Complement As Well. *Developmental Cell, 19*(3), 477-484. doi:10.1016/j.devcel.2010.08.005

Wingett, S. W., & Andrews, S. (2018). FastQ Screen: A tool for multi-genome mapping and quality control. *F1000Res, 7*, 1338. doi:10.12688/f1000research.15931.2

Yoshida, N., Yoshida, S., Koishi, K., Masuda, K., & Nabeshima, Y. (1998). Cell heterogeneity upon myogenic differentiation: down-regulation of MyoD and Myf-5 generates 'reserve cells'. *J Cell Sci, 111 (Pt 6)*, 769-779. doi:10.1242/jcs.111.6.769

Zacharewicz, E., Della Gatta, P., Reynolds, J., Garnham, A., Crowley, T., Russell, A. P., & Lamon, S. (2014). Identification of microRNAs linked to regulators of muscle protein synthesis and regeneration in young and old skeletal muscle. *PLoS One, 9*(12), e114009. doi:10.1371/journal.pone.0114009

Zacharewicz, E., Kalanon, M., Murphy, R. M., Russell, A. P., & Lamon, S. (2020). MicroRNA-99b-5p downregulates protein synthesis in human primary myotubes. *Am J Physiol Cell Physiol, 319*(2), C432-C440. doi:10.1152/ajpcell.00172.2020

Zore, T., Palafox, M., & Reue, K. (2018). Sex differences in obesity, lipid metabolism, and inflammation-A role for the sex chromosomes? *Mol Metab, 15*, 35-44. doi:10.1016/j.molmet.2018.04.003

The transcriptomic signature of age and sex is not conserved in human primary myocytes

Lamon S. et al.

Figures

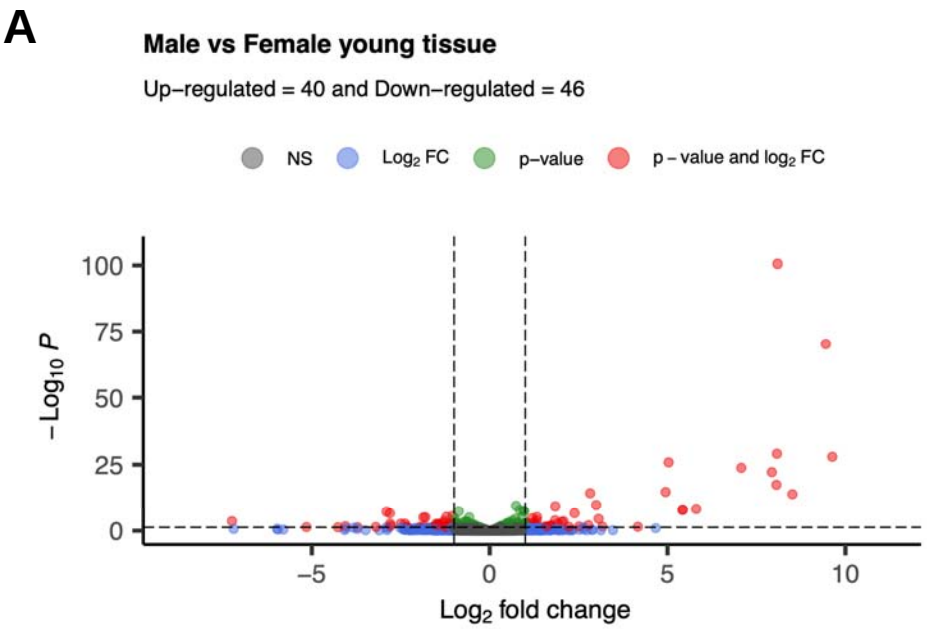
A
Male vs Female young tissue
Up−regulated = 40 and Down−regulated = 46
NS
Log2 FC
p−value
p − value and log2 FC
−Log10 P
Log2 fold change

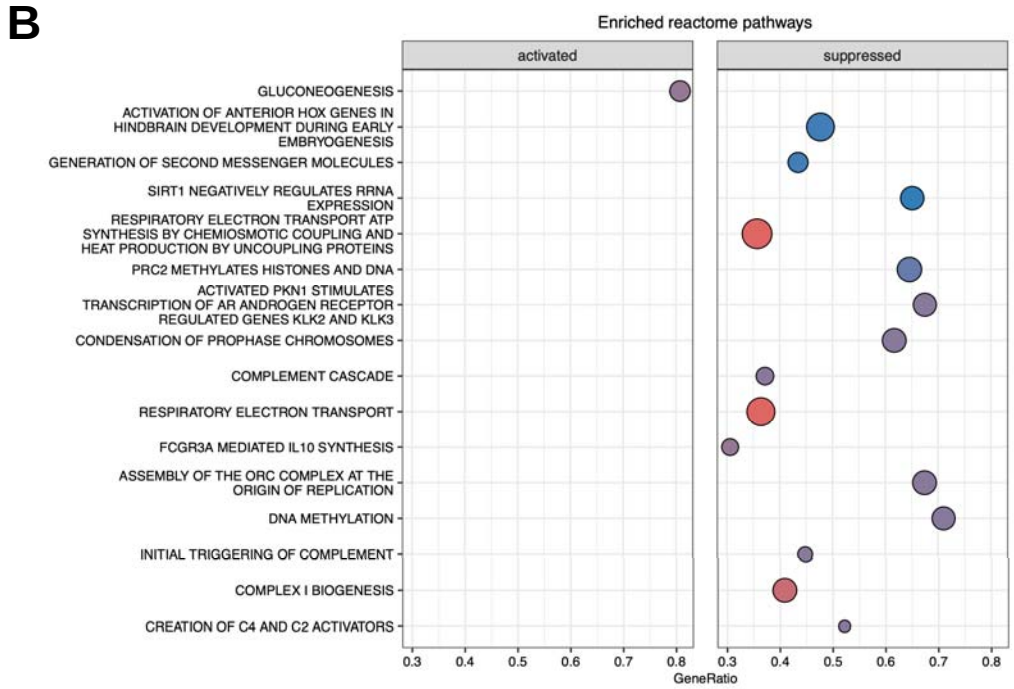
B
Enriched reactome pathways
activated
suppressed
GLUCONEOGENESIS
ACTIVATION OF ANTERIOR HOX GENES IN HINDBRAIN DEVELOPMENT DURING EARLY EMBRYOGENESIS
GENERATION OF SECOND MESSENGER MOLECULES
SIRT1 NEGATIVELY REGULATES RRNA EXPRESSION
RESPIRATORY ELECTRON TRANSPORT ATP SYNTHESIS BY CHEMIOSMOTIC COUPLING AND HEAT PRODUCTION BY UNCOUPLING PROTEINS
PRC2 METHYLATES HISTONES AND DNA
ACTIVATED PKN1 STIMULATES TRANSCRIPTION OF AR ANDROGEN RECEPTOR REGULATED GENES KLK2 AND KLK3
CONDENSATION OF PROPHASE CHROMOSOMES
COMPLEMENT CASCADE
RESPIRATORY ELECTRON TRANSPORT
FCGR3A MEDIATED IL10 SYNTHESIS
ASSEMBLY OF THE ORC COMPLEX AT THE ORIGIN OF REPLICATION
DNA METHYLATION
INITIAL TRIGGERING OF COMPLEMENT
COMPLEX I BIOGENESIS
CREATION OF C4 AND C2 ACTIVATORS
GeneRatio

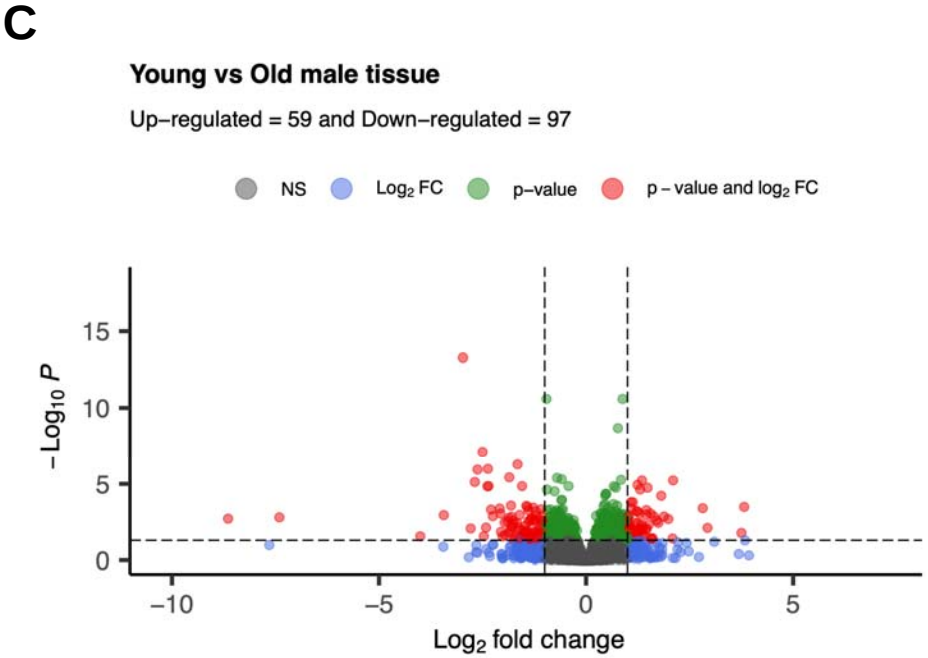
C
Young vs Old male tissue
Up−regulated = 59 and Down−regulated = 97
NS
Log2 FC
p−value
p − value and log2 FC
−Log10 P
Log2 fold change

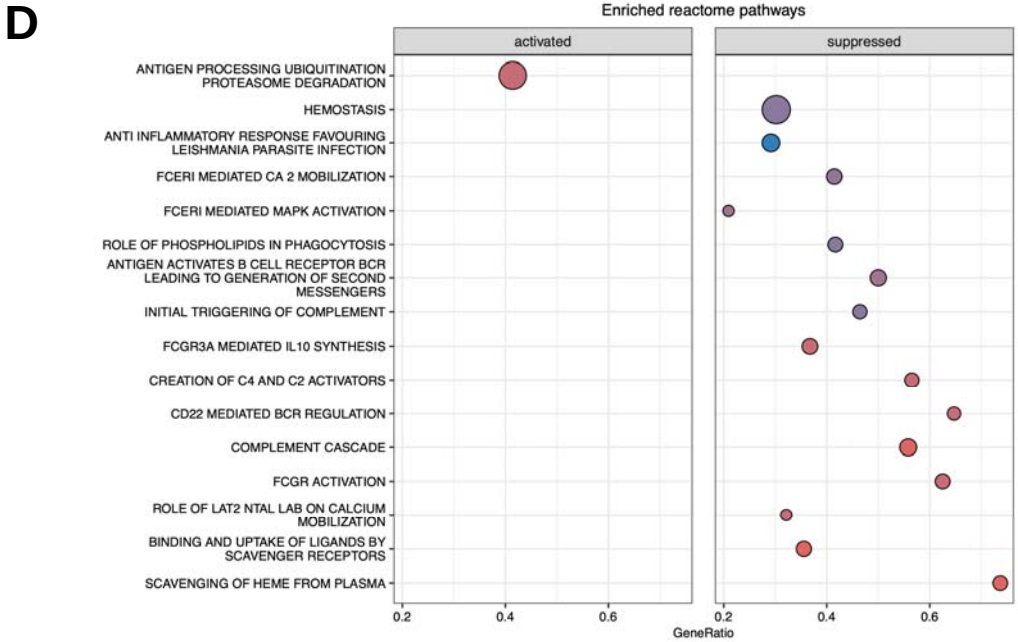
D
Enriched reactome pathways
activated
suppressed
ANTIGEN PROCESSING UBIQUITINATION PROTEASOME DEGRADATION
HEMOSTASIS
ANTI INFLAMMATORY RESPONSE FAVOURING LEISHMANIA PARASITE INFECTION
FCERI MEDIATED CA 2 MOBILIZATION
FCERI MEDIATED MAPK ACTIVATION
ROLE OF PHOSPHOLIPIDS IN PHAGOCYTOSIS
ANTIGEN ACTIVATES B CELL RECEPTOR BCR LEADING TO GENERATION OF SECOND MESSENGERS
INITIAL TRIGGERING OF COMPLEMENT
FCGR3A MEDIATED IL10 SYNTHESIS
CREATION OF C4 AND C2 ACTIVATORS
CD22 MEDIATED BCR REGULATION
COMPLEMENT CASCADE
FCGR ACTIVATION
ROLE OF LAT2 NTAL LAB ON CALCIUM MOBILIZATION
BINDING AND UPTAKE OF LIGANDS BY SCAVENGER RECEPTORS
SCAVENGING OF HEME FROM PLASMA
GeneRatio

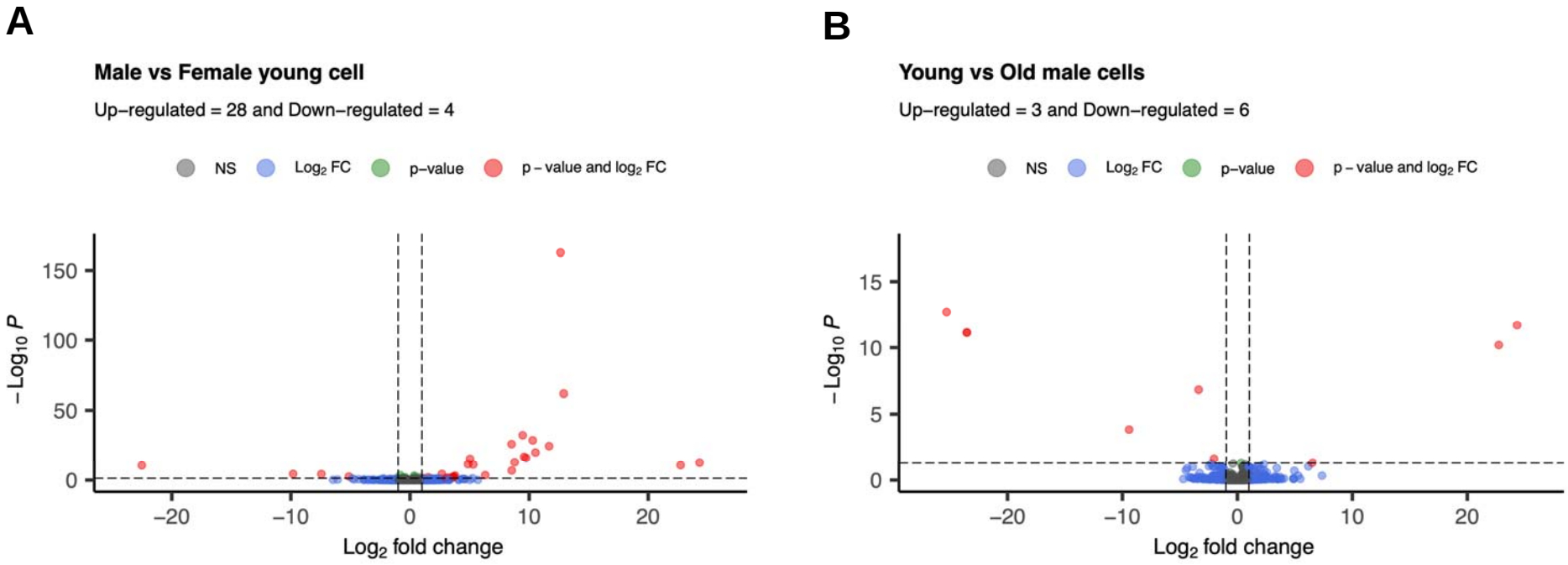
A
Male vs Female young cell
Up−regulated = 28 and Down−regulated = 4
NS
Log2 FC
p−value
p − value and log2 FC
−Log10 P
150
100
50
0
−20
−10
0
10
20
Log2 fold change
B
Young vs Old male cells
Up−regulated = 3 and Down−regulated = 6
NS
Log2 FC
p−value
p − value and log2 FC
−Log10 P
15
10
5
0
−20
−10
0
10
20
Log2 fold change

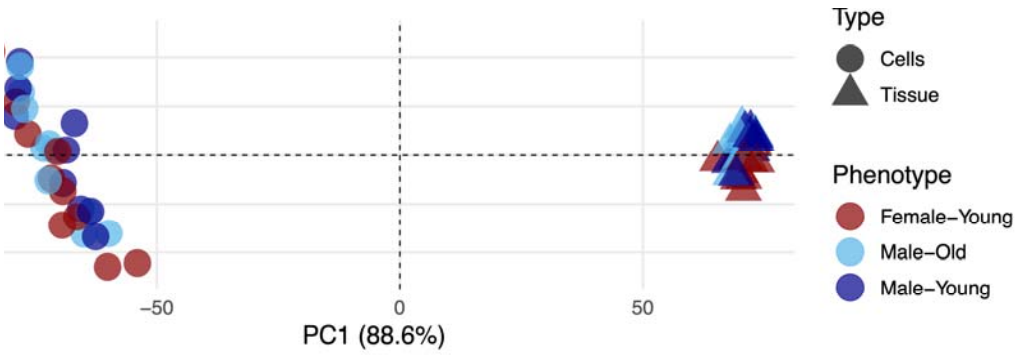
Type
Cells
Tissue
Phenotype
Female–Young
Male–Old
Male–Young
–50
0
50
PC1 (88.6%)

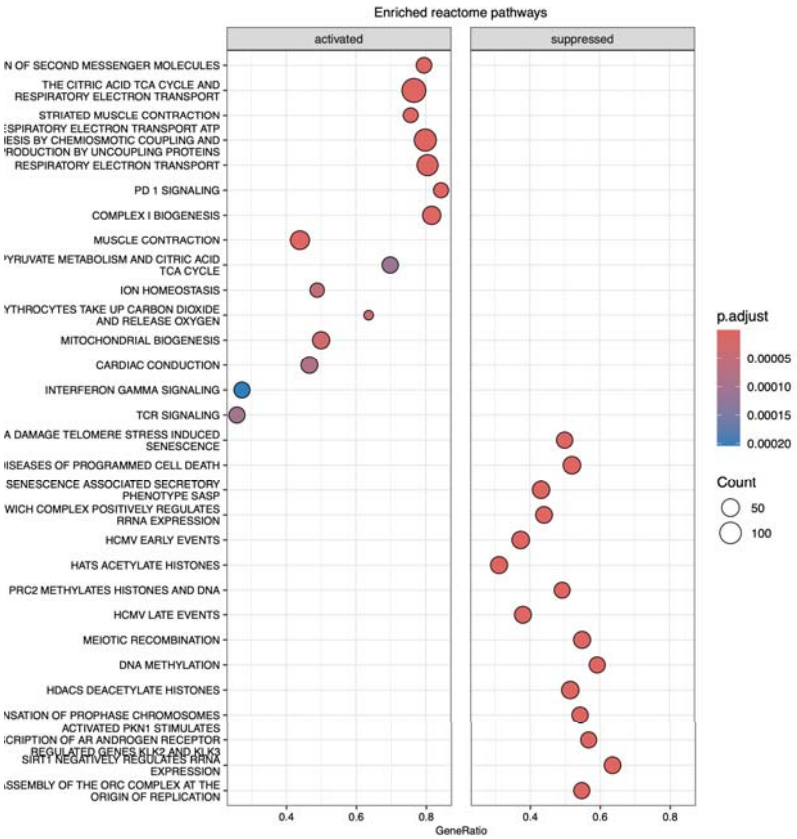
Enriched reactome pathways
activated
suppressed
N OF SECOND MESSENGER MOLECULES
THE CITRIC ACID TCA CYCLE AND RESPIRATORY ELECTRON TRANSPORT
STRIATED MUSCLE CONTRACTION
ESPIRATORY ELECTRON TRANSPORT ATP IESIS BY CHEMOSMOTIC COUPLING AND RODUCTION BY UNCOUPLING PROTEINS
RESPIRATORY ELECTRON TRANSPORT
PD 1 SIGNALING
COMPLEX I BIOGENESIS
MUSCLE CONTRACTION
YRUVATE METABOLISM AND CITRIC ACID TCA CYCLE
ION HOMEOSTASIS
YTHROCYTES TAKE UP CARBON DIOXIDE AND RELEASE OXYGEN
MITOCHONDRIAL BIOGENESIS
CARDIAC CONDUCTION
INTERFERON GAMMA SIGNALING
TCR SIGNALING
A DAMAGE TELOMERE STRESS INDUCED SENESCENCE
IISEASES OF PROGRAMMED CELL DEATH
SENESCENCE ASSOCIATED SECRETORY PHENOTYPE SASP
WICH COMPLEX POSITIVELY REGULATES RRNA EXPRESSION
HCMV EARLY EVENTS
HATS ACETYLATE HISTONES
PRC2 METHYLATES HISTONES AND DNA
HCMV LATE EVENTS
MEIOTIC RECOMBINATION
DNA METHYLATION
HDACS DEACETYLATE HISTONES
NSATION OF PROPHASE CHROMOSOMES
ACTIVATED PKN1 STIMULATES
CRIPTION OF AR ANDROGEN RECEPTOR REGULATED GENES KLK2 AND KLK3
SIRT1 NEGATIVELY REGULATES RRNA EXPRESSION
SSEMBLY OF THE ORC COMPLEX AT THE ORIGIN OF REPLICATION
0.4
0.6
0.8
GeneRatio
p.adjust
0.00005
0.00010
0.00015
0.00020
Count
50
100

B

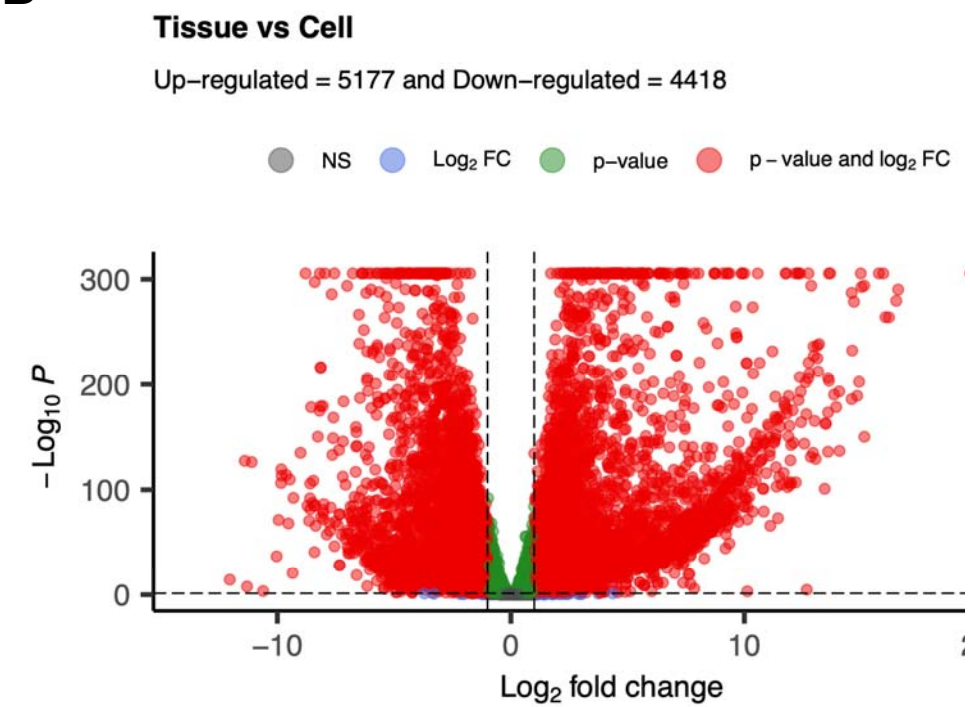
Tissue vs Cell
Up–regulated = 5177 and Down–regulated = 4418
NS
Log2 FC
p–value
p – value and log2 FC
300
200
100
0
– Log10 P
–10
0
10
Log2 fold change

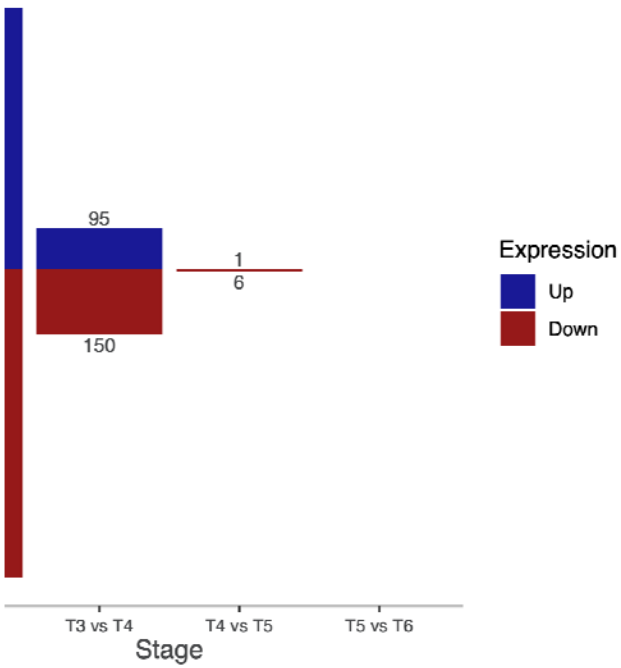
95
1
6
150
Expression
Up
Down
T3 vs T4
T4 vs T5
T5 vs T6
Stage

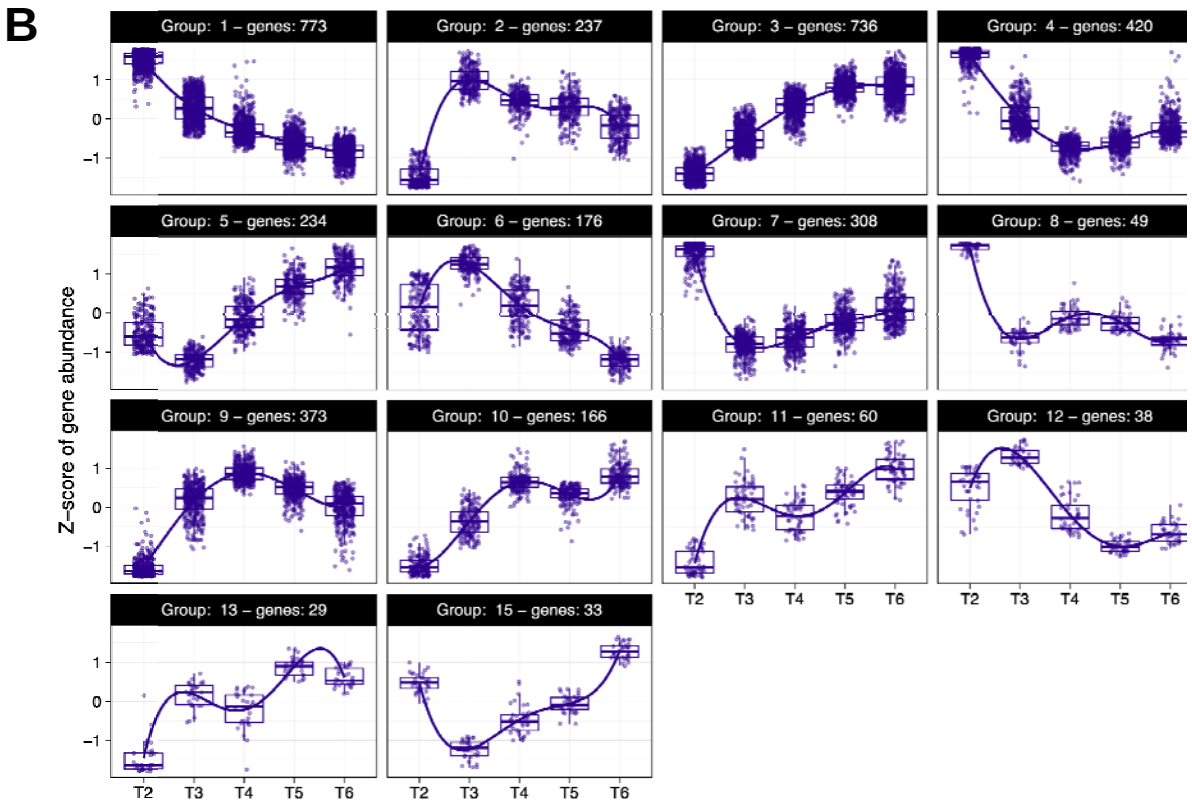
B
Group: 1 – genes: 773
Group: 2 – genes: 237
Group: 3 – genes: 736
Group: 4 – genes: 420
Group: 5 – genes: 234
Group: 6 – genes: 176
Group: 7 – genes: 308
Group: 8 – genes: 49
Group: 9 – genes: 373
Group: 10 – genes: 166
Group: 11 – genes: 60
Group: 12 – genes: 38
Group: 13 – genes: 29
Group: 15 – genes: 33
Z–score of gene abundance
T2
T3
T4
T5
T6

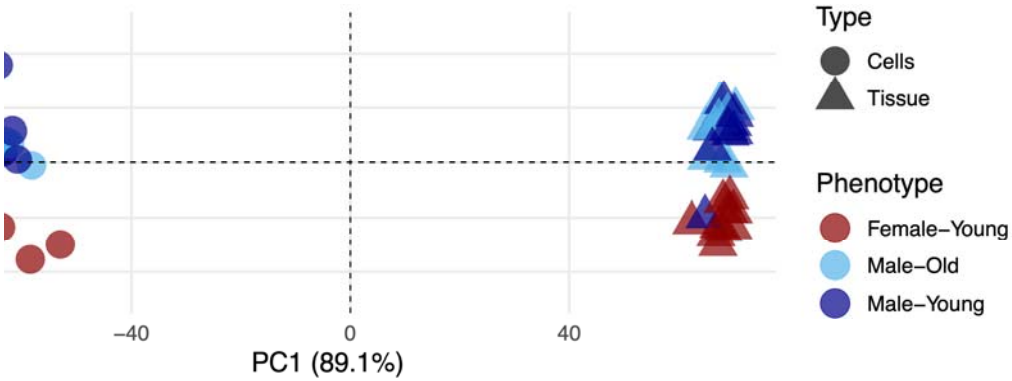
Type
Cells
Tissue
Phenotype
Female–Young
Male–Old
Male–Young
–40
0
40
PC1 (89.1%)

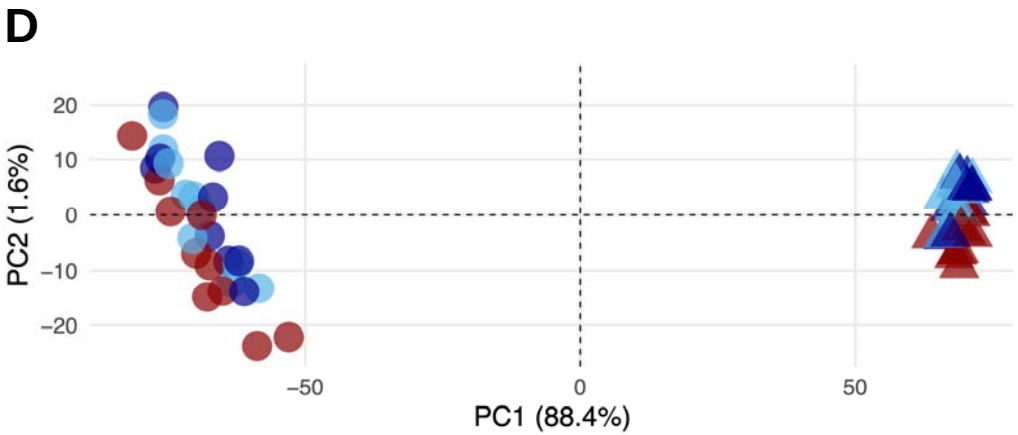
D
PC2 (1.6%)
20
10
0
–10
–20
–50
0
50
PC1 (88.4%)

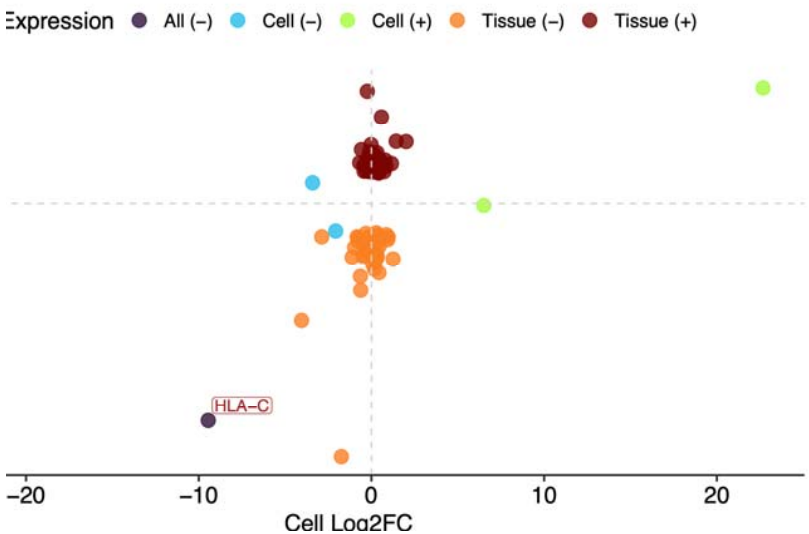
Expression
All (−)
Cell (−)
Cell (+)
Tissue (−)
Tissue (+)
HLA−C
−20
−10
0
10
20
Cell Log2FC

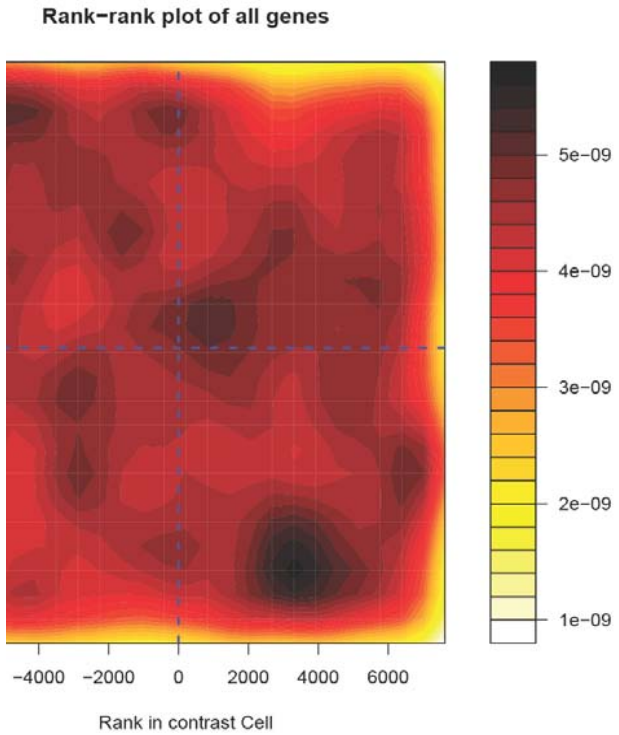
Rank−rank plot of all genes
5e−09
4e−09
3e−09
2e−09
1e−09
−4000
−2000
0
2000
4000
6000
Rank in contrast Cell

C

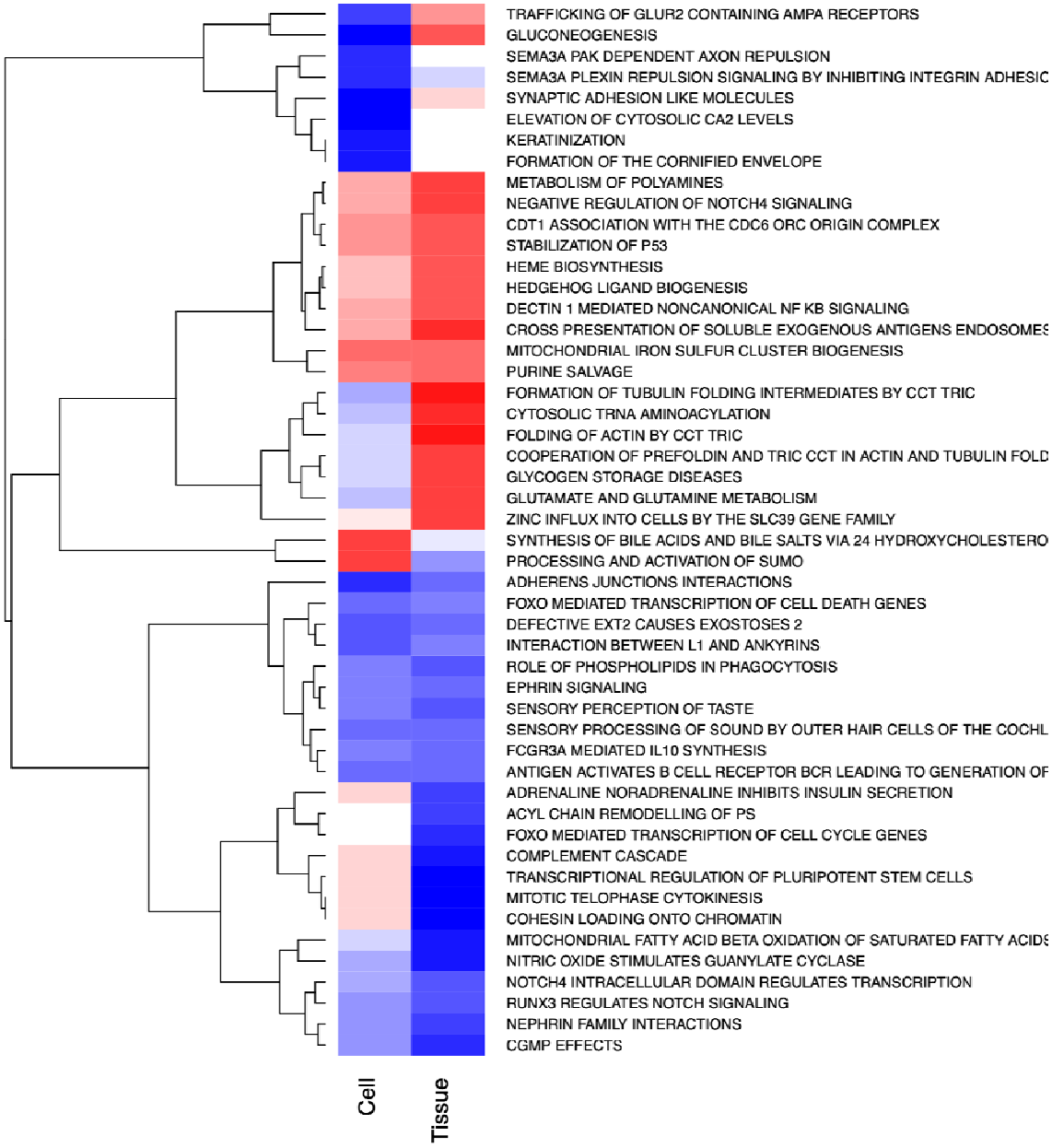
TRAFFICKING OF GLUR2 CONTAINING AMPA RECEPTORS
GLUCONEOGENESIS
SEMA3A PAK DEPENDENT AXON REPULSION
SEMA3A PLEXIN REPULSION SIGNALING BY INHIBITING INTEGRIN ADHESIC
SYNAPTIC ADHESION LIKE MOLECULES
ELEVATION OF CYTOSOLIC CA2 LEVELS
KERATINIZATION
FORMATION OF THE CORNIFIED ENVELOPE
METABOLISM OF POLYAMINES
NEGATIVE REGULATION OF NOTCH4 SIGNALING
CDT1 ASSOCIATION WITH THE CDC6 ORC ORIGIN COMPLEX
STABILIZATION OF P53
HEME BIOSYNTHESIS
HEDGEHOG LIGAND BIOGENESIS
DECTIN 1 MEDIATED NONCANONICAL NF KB SIGNALING
CROSS PRESENTATION OF SOLUBLE EXOGENOUS ANTIGENS ENDOSOMES
MITOCHONDRIAL IRON SULFUR CLUSTER BIOGENESIS
PURINE SALVAGE
FORMATION OF TUBULIN FOLDING INTERMEDIATES BY CCT TRIC
CYTOSOLIC TRNA AMINOACYLATION
FOLDING OF ACTIN BY CCT TRIC
COOPERATION OF PREFOLDIN AND TRIC CCT IN ACTIN AND TUBULIN FOLD
GLYCOGEN STORAGE DISEASES
GLUTAMATE AND GLUTAMINE METABOLISM
ZINC INFLUX INTO CELLS BY THE SLC39 GENE FAMILY
SYNTHESIS OF BILE ACIDS AND BILE SALTS VIA 24 HYDROXYCHOLESTERO
PROCESSING AND ACTIVATION OF SUMO
ADHERENS JUNCTIONS INTERACTIONS
FOXO MEDIATED TRANSCRIPTION OF CELL DEATH GENES
DEFECTIVE EXT2 CAUSES EXOSTOSES 2
INTERACTION BETWEEN L1 AND ANKYRINS
ROLE OF PHOSPHOLIPIDS IN PHAGOCYTOSIS
EPHRIN SIGNALING
SENSORY PERCEPTION OF TASTE
SENSORY PROCESSING OF SOUND BY OUTER HAIR CELLS OF THE COCHL
FCGR3A MEDIATED IL10 SYNTHESIS
ANTIGEN ACTIVATES B CELL RECEPTOR BCR LEADING TO GENERATION OF
ADRENALINE NORADRENALINE INHIBITS INSULIN SECRETION
ACYL CHAIN REMODELLING OF PS
FOXO MEDIATED TRANSCRIPTION OF CELL CYCLE GENES
COMPLEMENT CASCADE
TRANSCRIPTIONAL REGULATION OF PLURIPOTENT STEM CELLS
MITOTIC TELOPHASE CYTOKINESIS
COHESIN LOADING ONTO CHROMATIN
MITOCHONDRIAL FATTY ACID BETA OXIDATION OF SATURATED FATTY ACIDS
NITRIC OXIDE STIMULATES GUANYLATE CYCLASE
NOTCH4 INTRACELLULAR DOMAIN REGULATES TRANSCRIPTION
RUNX3 REGULATES NOTCH SIGNALING
NEPHRIN FAMILY INTERACTIONS
CGMP EFFECTS
Cell
Tissue

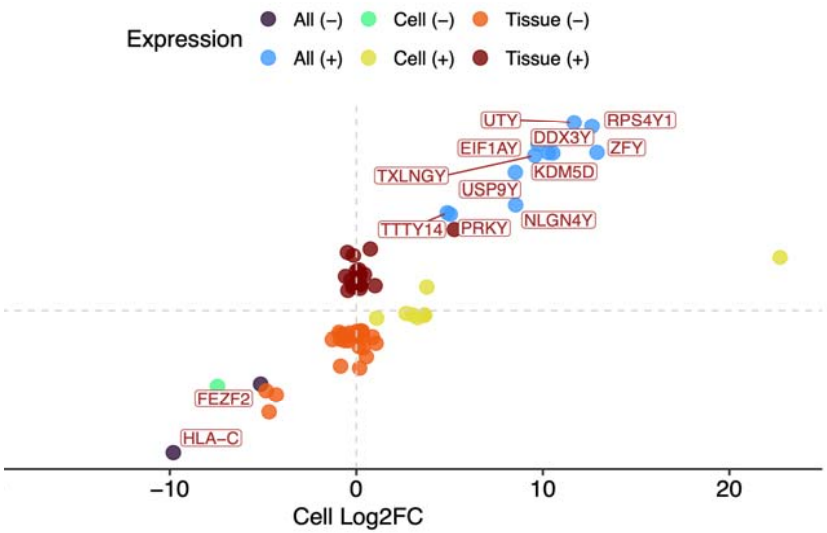
Expression
All (−)
Cell (−)
Tissue (−)
All (+)
Cell (+)
Tissue (+)
UTY
RPS4Y1
DDX3Y
EIF1AY
ZFY
TXLNGY
KDM5D
USP9Y
TTTY14
PRKY
NLGN4Y
FEZF2
HLA−C
−10
0
10
20
Cell Log2FC

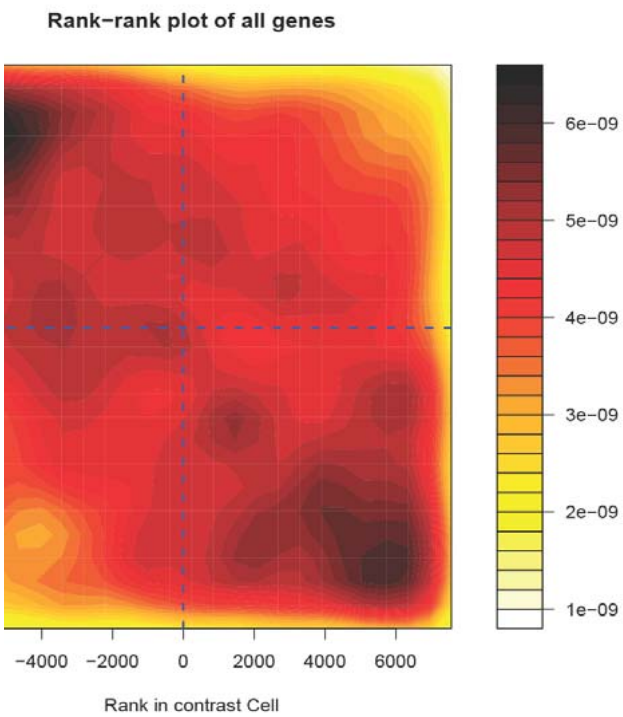
Rank−rank plot of all genes
6e−09
5e−09
4e−09
3e−09
2e−09
1e−09
−4000
−2000
0
2000
4000
6000
Rank in contrast Cell

C

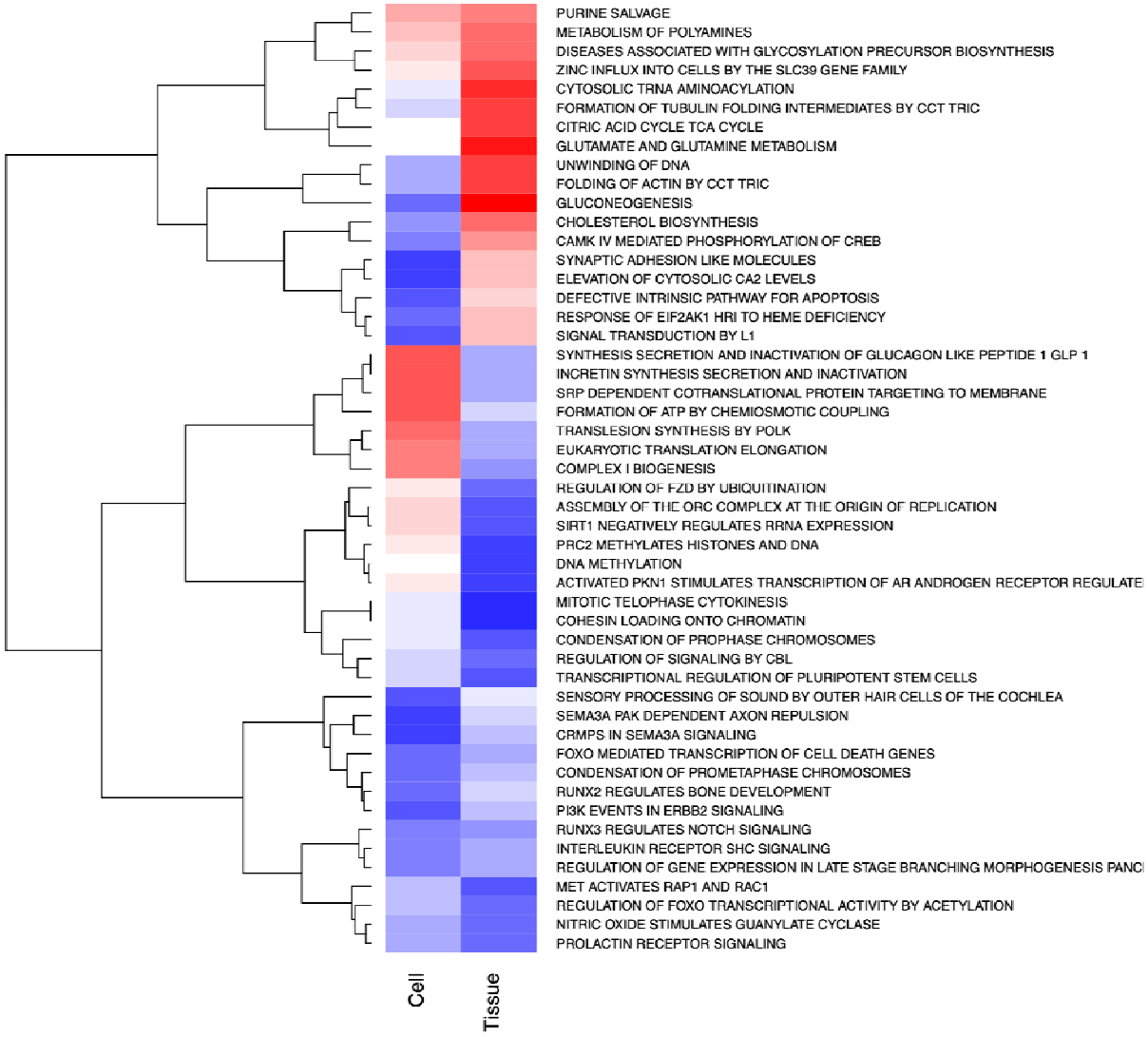
PURINE SALVAGE
METABOLISM OF POLYAMINES
DISEASES ASSOCIATED WITH GLYCOSYLATION PRECURSOR BIOSYNTHESIS
ZINC INFLUX INTO CELLS BY THE SLC39 GENE FAMILY
CYTOSOLIC TRNA AMINOACYLATION
FORMATION OF TUBULIN FOLDING INTERMEDIATES BY CCT TRIC
CITRIC ACID CYCLE TCA CYCLE
GLUTAMATE AND GLUTAMINE METABOLISM
UNWINDING OF DNA
FOLDING OF ACTIN BY CCT TRIC
GLUCONEOGENESIS
CHOLESTEROL BIOSYNTHESIS
CAMK IV MEDIATED PHOSPHORYLATION OF CREB
SYNAPTIC ADHESION LIKE MOLECULES
ELEVATION OF CYTOSOLIC CA2 LEVELS
DEFECTIVE INTRINSIC PATHWAY FOR APOPTOSIS
RESPONSE OF EIF2AK1 HRI TO HEME DEFICIENCY
SIGNAL TRANSDUCTION BY L1
SYNTHESIS SECRETION AND INACTIVATION OF GLUCAGON LIKE PEPTIDE 1 GLP 1
INCRETIN SYNTHESIS SECRETION AND INACTIVATION
SRP DEPENDENT COTRANSLATIONAL PROTEIN TARGETING TO MEMBRANE
FORMATION OF ATP BY CHEMIOSMOTIC COUPLING
TRANSLESION SYNTHESIS BY POLK
EUKARYOTIC TRANSLATION ELONGATION
COMPLEX I BIOGENESIS
REGULATION OF FZD BY UBIQUITINATION
ASSEMBLY OF THE ORC COMPLEX AT THE ORIGIN OF REPLICATION
SIRT1 NEGATIVELY REGULATES RRNA EXPRESSION
PRC2 METHYLATES HISTONES AND DNA
DNA METHYLATION
ACTIVATED PKN1 STIMULATES TRANSCRIPTION OF AR ANDROGEN RECEPTOR REGULATE
MITOTIC TELOPHASE CYTOKINESIS
COHESIN LOADING ONTO CHROMATIN
CONDENSATION OF PROPHASE CHROMOSOMES
REGULATION OF SIGNALING BY CBL
TRANSCRIPTIONAL REGULATION OF PLURIPOTENT STEM CELLS
SENSORY PROCESSING OF SOUND BY OUTER HAIR CELLS OF THE COCHLEA
SEMA3A PAK DEPENDENT AXON REPULSION
CRMPS IN SEMA3A SIGNALING
FOXO MEDIATED TRANSCRIPTION OF CELL DEATH GENES
CONDENSATION OF PROMETAPHASE CHROMOSOMES
RUNX2 REGULATES BONE DEVELOPMENT
PI3K EVENTS IN ERBB2 SIGNALING
RUNX3 REGULATES NOTCH SIGNALING
INTERLEUKIN RECEPTOR SHC SIGNALING
REGULATION OF GENE EXPRESSION IN LATE STAGE BRANCHING MORPHOGENESIS PANC
MET ACTIVATES RAP1 AND RAC1
REGULATION OF FOXO TRANSCRIPTIONAL ACTIVITY BY ACETYLATION
NITRIC OXIDE STIMULATES GUANYLATE CYCLASE
PROLACTIN RECEPTOR SIGNALING
Cell
Tissue

nentary Figure 1

B

C

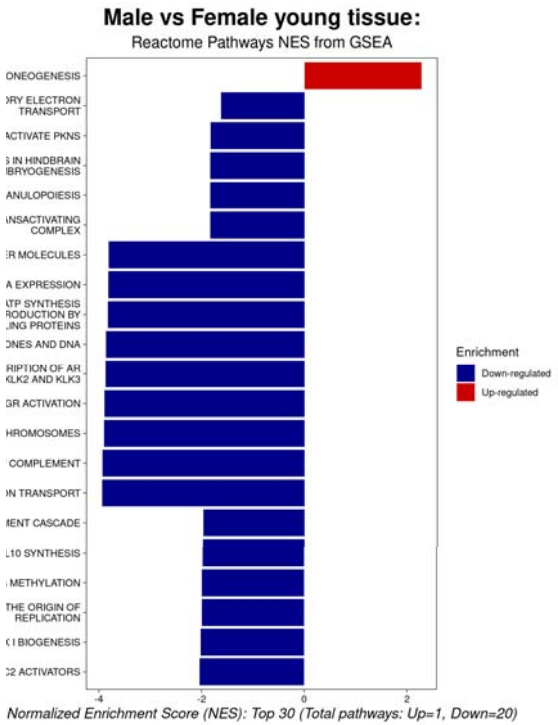

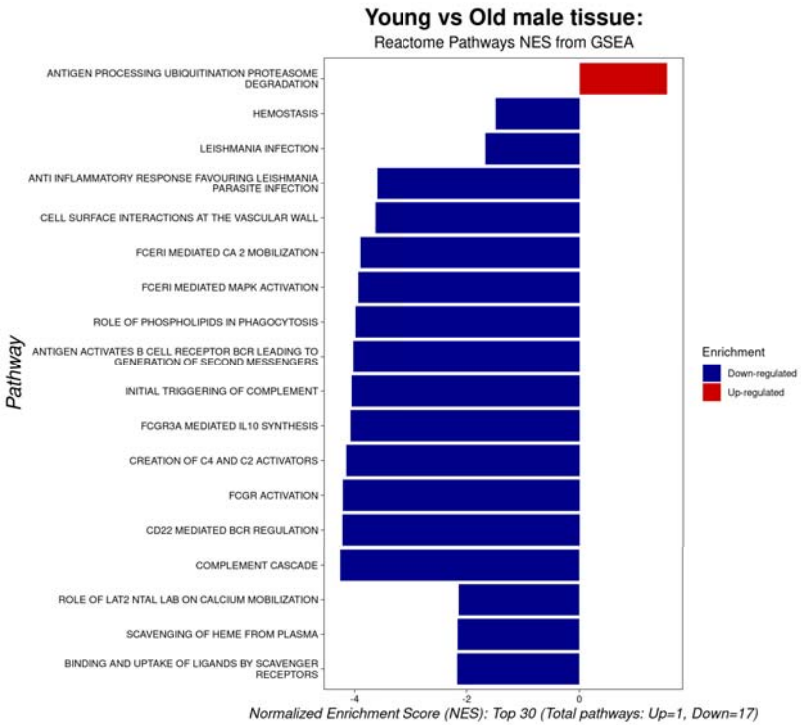

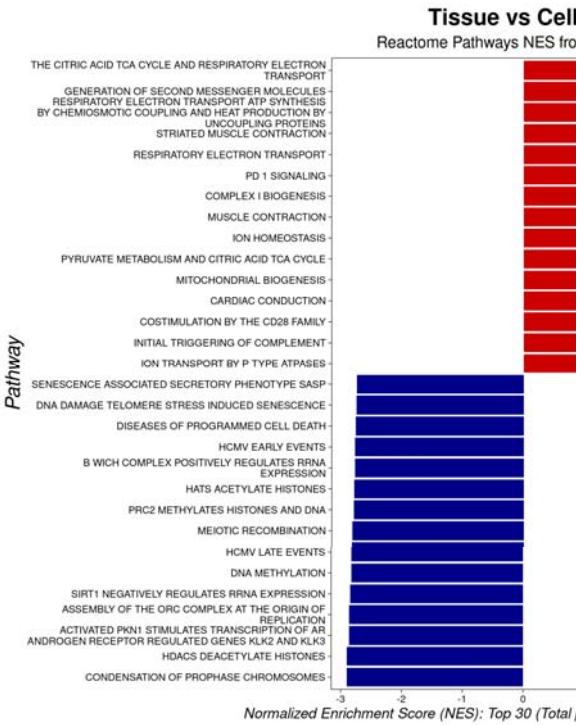

nentary Figure 2 (1/4)

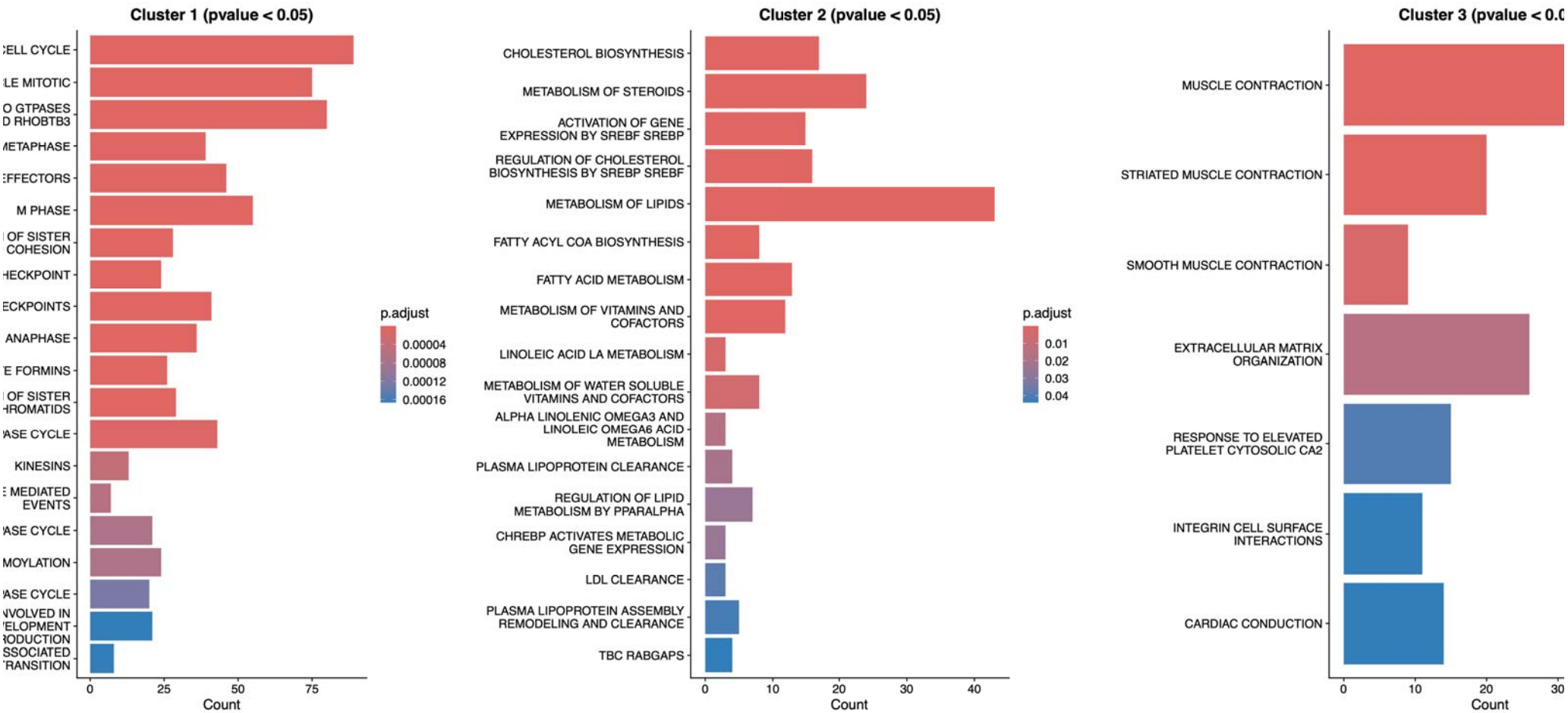

nentary Figure 2 (2/4)

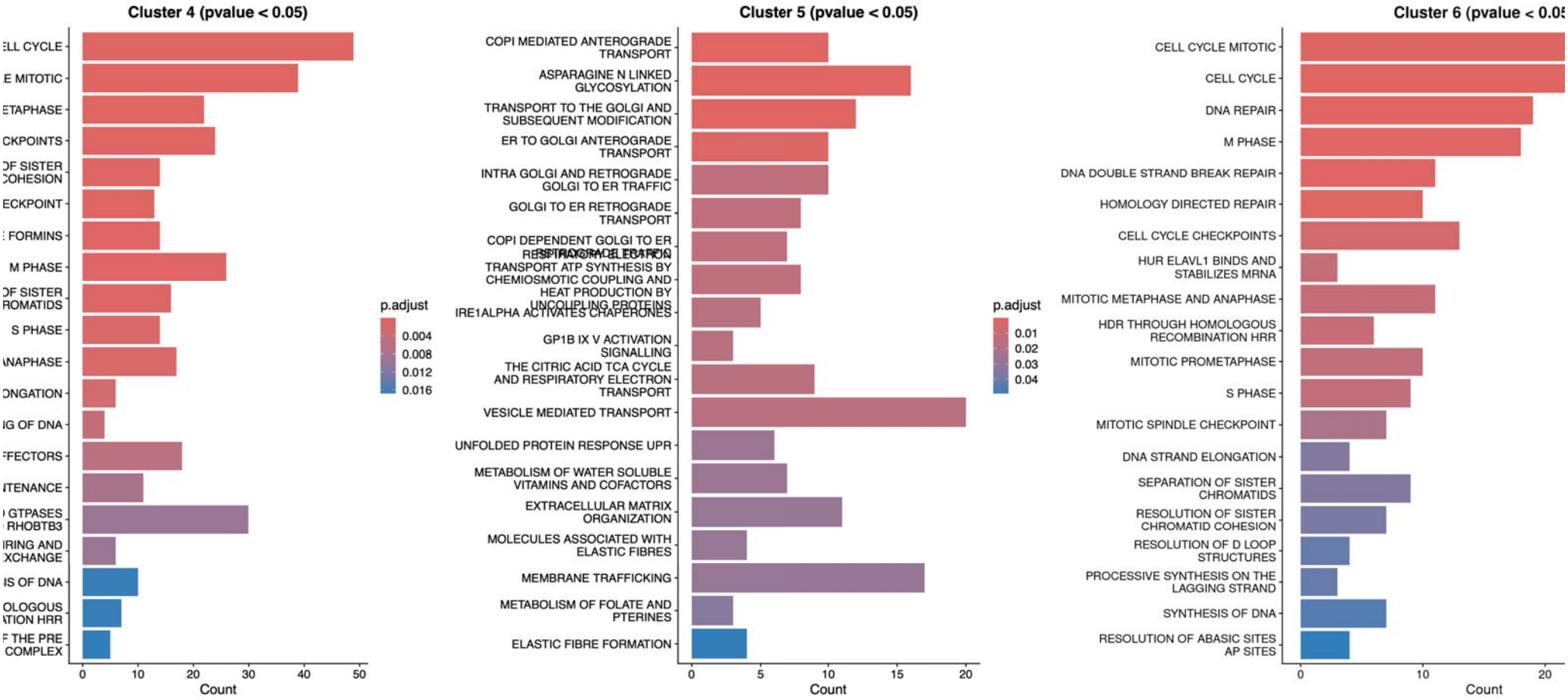

nentary Figure 2 (3/4)

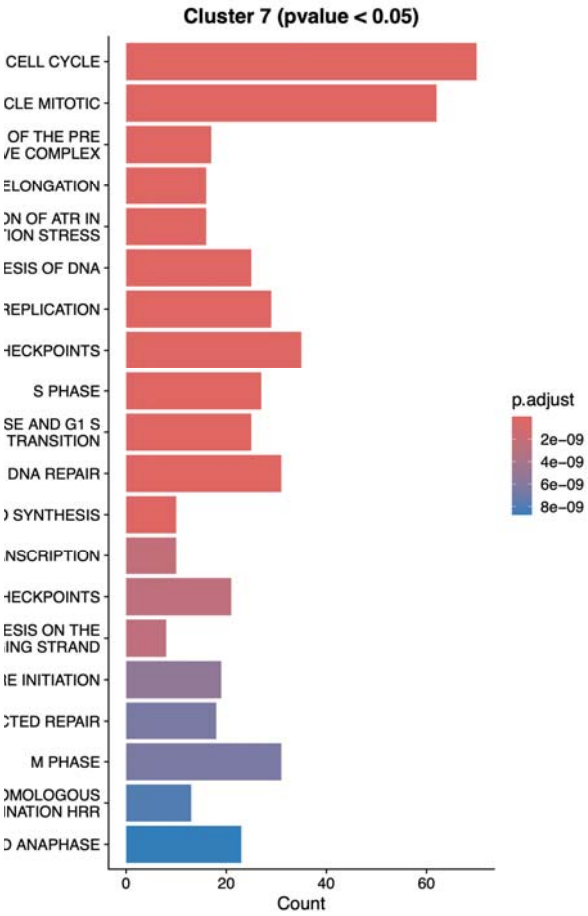

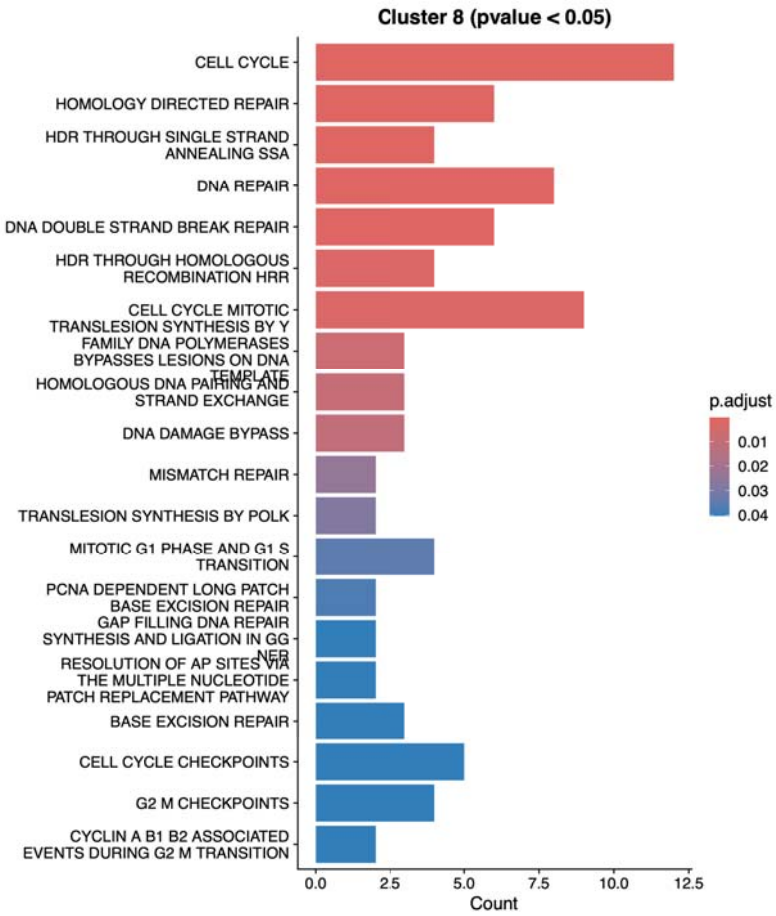

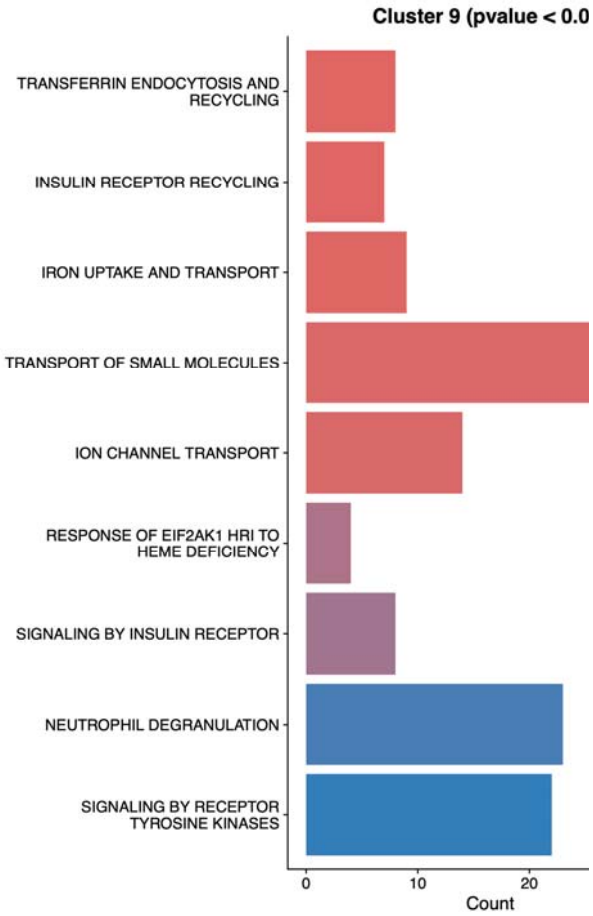

nentary Figure 2 (4/4)

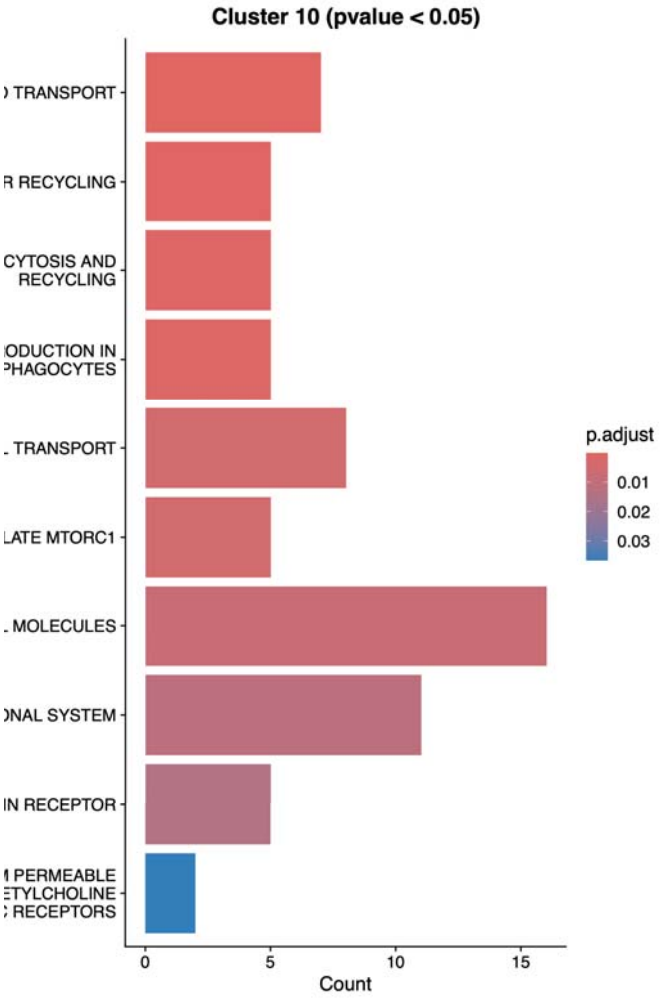

nentary Figure 3

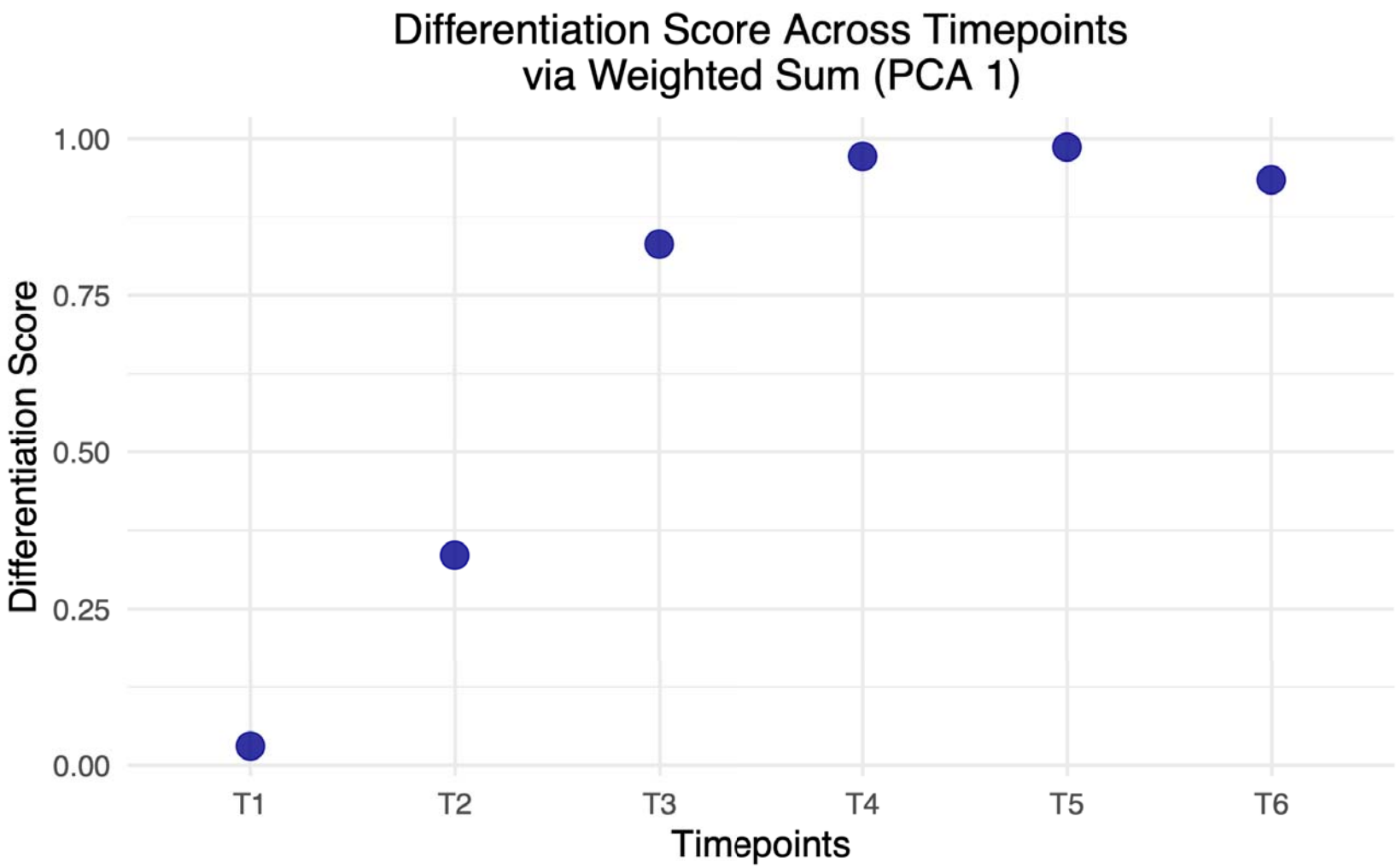

nentary Figure 4

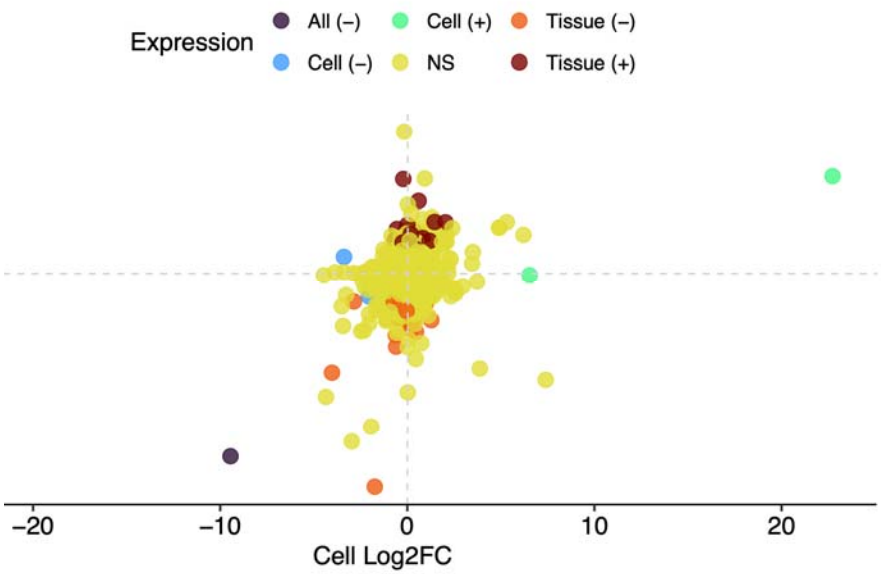
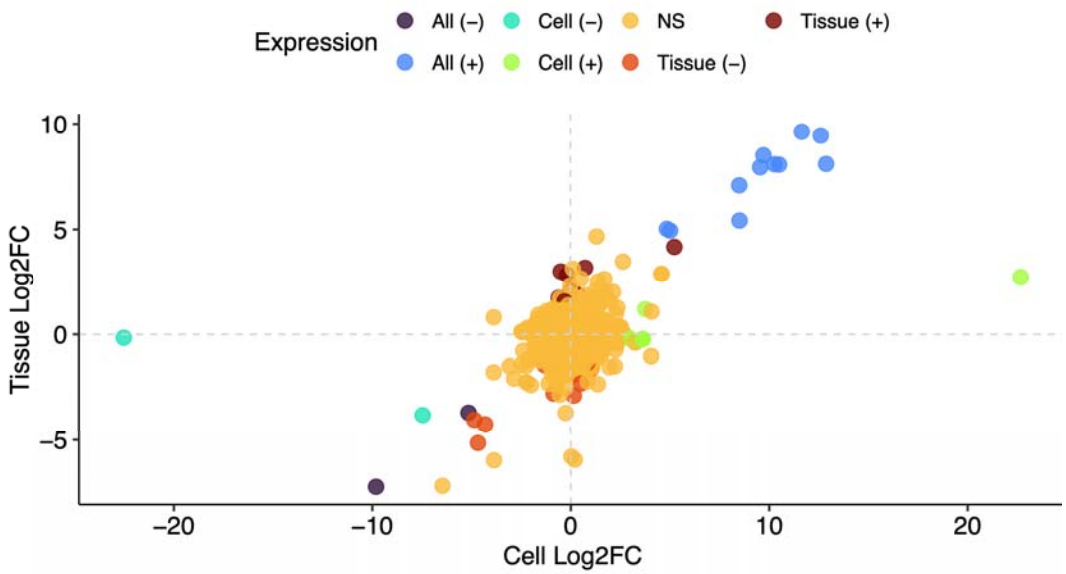
B